



8-2014

## **Statistical Mechanics and Schramm-Loewner Evolution with Applications to Crack Propagation Processes**

Christopher Borut Mesic

*University of Tennessee - Knoxville, [cmesic@vols.utk.edu](mailto:cmesic@vols.utk.edu)*

Follow this and additional works at: [https://trace.tennessee.edu/utk\\_gradthes](https://trace.tennessee.edu/utk_gradthes)



Part of the [Analysis Commons](#), [Numerical Analysis and Computation Commons](#), and the [Probability Commons](#)

---

### **Recommended Citation**

Mesic, Christopher Borut, "Statistical Mechanics and Schramm-Loewner Evolution with Applications to Crack Propagation Processes. " Master's Thesis, University of Tennessee, 2014.  
[https://trace.tennessee.edu/utk\\_gradthes/2832](https://trace.tennessee.edu/utk_gradthes/2832)

This Thesis is brought to you for free and open access by the Graduate School at TRACE: Tennessee Research and Creative Exchange. It has been accepted for inclusion in Masters Theses by an authorized administrator of TRACE: Tennessee Research and Creative Exchange. For more information, please contact [trace@utk.edu](mailto:trace@utk.edu).

To the Graduate Council:

I am submitting herewith a thesis written by Christopher Borut Mesic entitled "Statistical Mechanics and Schramm-Loewner Evolution with Applications to Crack Propagation Processes." I have examined the final electronic copy of this thesis for form and content and recommend that it be accepted in partial fulfillment of the requirements for the degree of Master of Science, with a major in Mathematics.

Joan R. Lind, Major Professor

We have read this thesis and recommend its acceptance:

Michael W. Frazier, Suzanne M. Lenhart

Accepted for the Council:

Carolyn R. Hodges

Vice Provost and Dean of the Graduate School

(Original signatures are on file with official student records.)

# **Statistical Mechanics and Schramm-Loewner Evolution with Applications to Crack Propagation Processes**

A Thesis Presented for the

Master of Science

Degree

The University of Tennessee, Knoxville

Christopher Borut Mesic

August 2014

© by Christopher Borut Mesic, 2014  
All Rights Reserved.

*Dedicated to my supportive and loving parents*

# Acknowledgements

I would like to thank Betsy Heines and Josh Lipsmeyer for their outstanding support, patience, kindness, and consultation throughout my graduate career. I would also like to thank all the members of my committee for their support and patience. I would especially like to thank my eternally patient advisor, who encouraged me to pursue this idea, and gave me the support I needed throughout this long process.

# Abstract

Schramm-Loewner Evolution (SLE) has both mathematical and physical roots that extend as far back as the early 20th century. We present the progression of these humble roots from the Ideal Gas Law, all the way to the renormalization group and conformal field theory, to better understand the impact SLE has had on modern statistical mechanics. We then explore the potential application of the percolation exploration process to crack propagation processes, illustrating the interplay between mathematics and physics.

# Table of Contents

<b>1</b>	<b>Introduction</b>	<b>1</b>
<b>2</b>	<b>Motivational Physics</b>	<b>4</b>
2.1	Physical Context . . . . .	4
2.2	The Ising Model . . . . .	8
2.3	Advanced Physics . . . . .	20
<b>3</b>	<b>Introduction to Schramm-Loewner Evolution Concepts</b>	<b>27</b>
3.1	Schramm-Loewner Evolution . . . . .	27
<b>4</b>	<b>Crack Propagation Application</b>	<b>36</b>
4.1	The Percolation Model . . . . .	36
4.2	Crack Propagation Simulations . . . . .	37
<b>5</b>	<b>Conclusions</b>	<b>43</b>
	<b>Bibliography</b>	<b>45</b>
	<b>Appendix</b>	<b>48</b>
	<b>Vita</b>	<b>66</b>



# List of Figures

Figure 2.1:	$H_2O$ phase diagram . . . . .	5
Figure 2.2:	Guggenheim plot . . . . .	7
Figure 2.3:	$\Delta\rho$ order parameter plot . . . . .	9
Figure 2.4:	1-D Ising set-up . . . . .	10
Figure 2.5:	2-D Ising set-up . . . . .	11
Figure 2.6:	Average magnetization . . . . .	13
Figure 2.7:	Magnetic susceptibility . . . . .	13
Figure 2.8:	Ising model order parameters . . . . .	14
Figure 2.9:	Numerical simulation of Ising model . . . . .	15
Figure 2.10:	Temp vs Avg.Mag 1 . . . . .	18
Figure 2.11:	Temp vs Avg. Mag 2 . . . . .	18
Figure 2.12:	Temp vs Avg. Mag 3 . . . . .	19
Figure 2.13:	Coarse-Graining . . . . .	22
Figure 2.14:	Physics Recap . . . . .	26
Figure 3.1:	2-D random walk . . . . .	29
Figure 3.2:	2-D loop-erased random walk . . . . .	30
Figure 3.3:	Zero driving function . . . . .	32
Figure 3.4:	SLE(6) . . . . .	34
Figure 3.5:	SLE(2) . . . . .	34
Figure 3.6:	Ising model SLE(3) . . . . .	35
Figure 4.1:	Percolation model . . . . .	37
Figure 4.2:	Percolation model inspiration . . . . .	38

Figure 4.3:	Crack process inspiration . . . . .	38
Figure 4.4:	Failings of the percolation model . . . . .	39
Figure 4.5:	Small scale pinch process . . . . .	40
Figure 4.6:	Large scale pinch process . . . . .	41
Figure 4.7:	Large scale comparison . . . . .	42

# List of Tables

Table 2.1: Comparison of Ising model data . . . . .	20
---	----

# Chapter 1

## Introduction

Schramm-Loewner Evolution has a lengthy history characterized not by its rapid rise or immediate consequences, but rather by quiet decades of solitary anticipation, accented with moments of discovery which coalesced during auspicious circumstances to yield a uniquely innovative mathematical formalism. Mathematically, the roots of Schramm-Loewner Evolution (SLE) are found in the Bieberbach conjecture. This was only half of the story however, as the need for physicists to rigorously justify their numerical simulations proved to be the impetus for the other half of SLE's inception.

The Bieberbach conjecture, which states that every conformal map  $f(z) = \sum_{n=1}^{\infty} a_n z^n$  defined on the unit disc satisfies  $|a_n| \leq n|a_1|$  [6], was studied extensively by mathematicians in the early 20th century, and Charles Loewner was one such mathematician. Charles Loewner received his PhD from the University of Prague in the Czech Republic. Loewner immigrated to the US during the onset of World War II to escape Nazi persecution, having been born to a Jewish family. Loewner went on to much acclaim and success at Brown University, Syracuse and ultimately Stanford University. It was Loewner's work on the Bieberbach conjecture that would be of renewed interest in the early part of 21st century.

Loewner proved a particular case of the Birberbach conjecture using a differential equation he invented, now known as the Loewner equation. Many years later, Oded

Schramm used Loewner’s differential equation in a probabilistic context. Schramm named his process Stochastic-Loewner Evolution, but it soon became known as Schramm-Loewner Evolution (SLE) as a tribute to Oded Schramm, who died in 2008. Schramm’s discovery was met with much praise. Two fellow mathematicians, Stanislav Smirnov and Wendelin Werner who helped Schramm develop SLE, were later awarded the Fields Medal for their contributions. Unfortunately, Schramm was excluded due to an age eligibility stipulation for the Fields Medal.

Schramm-Loewner Evolution found exciting applications to problems in statistical mechanics and quantum physics; for instance, the application of SLE to the percolation process through materials. In general, SLE has proven most applicable to physical problems demanding a scaling limit. Essentially, SLE has the unique ability to accurately translate complicated problems in some continuous space to a well understood discrete space, where explicit calculations and analysis are generally more manageable. Ongoing research of SLE promises more exciting applications, including but certainly not limited to: Turbulent fluid flow, crystalline structure, and planar circle packing. As the journey of discovery continues for SLE, the future looks more promising than ever.

## **Thesis Structure**

This thesis is divided into three sections. The first section, chapter 2, is designed to provide a mathematically inclined reader some physical context for the motivation and creation of SLE. We explore the evolution of statistical mechanics and see how SLE can provide additional insight and address fundamental questions about certain models. In particular, we introduce and explore the Ising model to illustrate basic statistical mechanics concepts. Additionally, we provide a non-rigorous introduction to conformal field theory, the renormalization group and note their contributions to the development of lattice models in statistical mechanics as well as their deficiencies. This motivates the second section of the thesis in chapter 3, where a more technical

introduction to SLE is given, including a brief introduction of some of the relevant probabilistic concepts. The chapter concludes with a description of the connection between SLE and certain physical models. The last section of the thesis, chapters 4 and 5, pertain to the exploration of a model for crack propagation processes. We discuss our motivation and model choice, as well as the algorithm we wrote to implement our ideas. We conclude this section and the thesis with our results, potential improvements, and future work.

# Chapter 2

## Motivational Physics

### 2.1 Physical Context

As the title of this chapter implies, we hope to provide sufficient physical motivation for SLE, and perhaps more importantly, to develop some context for that motivation. This requires us to first consider the fundamental physical question being asked, and then examine the progression of its solutions. The question physicists sought to answer was simple: How does matter transition between its phases of solid, liquid, and gas? The most common example of a phase transition is ice melting into liquid water, or water boiling into steam. Although a simple question, years of study would reveal a very complicated, chaotic and poorly understood process. It is at the end of this process that SLE will provide a compelling alternative to past mathematical descriptions and yield new insights to this old question.

The first step in this process is to become familiar with some of the basic terminology and concepts of phase transitions. This is easiest by looking at a phase diagram, a visual tool used to illustrate the relationship between various physical properties, typically temperature and pressure. Figure (2.1) is a basic phase diagram for the molecule of water. We see the now familiar phenomena of boiling and freezing points dividing the diagram into the ice, water, and steam sections. A point that

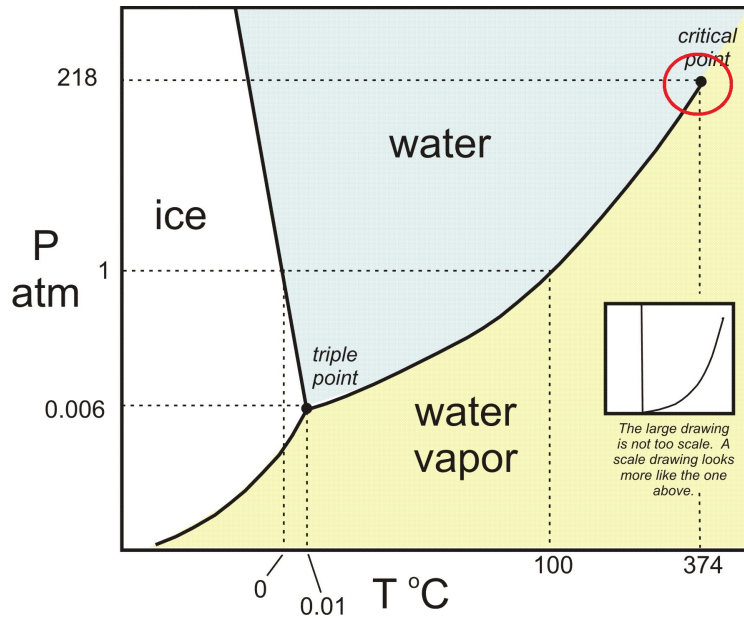


**Figure 2.1:** Phase diagram of water courtesy David Mogk

will become of interest later is the critical point. This is the point at the end of the liquid-gas coexistence curve, where we see at high enough temperatures, the liquid and gas phases of water become indistinguishable, regardless of pressure. We will go over that in more detail later. Now that we are familiar with the basics we can proceed with the first attempts to quantify the interaction of these various physical properties.

## The Ideal Gas Law

Physicist and chemists wanted to try and understand how transitions took place and how these transitions affected various properties of matter. When water boils and turns into steam, what happens to the temperature, pressure, and volume? The first attempt to mathematically encapsulate these properties and their interaction was the Ideal Gas Law proposed in 1834. The law is quite simple and can be stated as follows:

$$PV = nRT$$



where  $P, V, T$  are pressure, volume, and temperature respectively. The remaining terms,  $R, n$  are the ideal gas constant and the number of moles of the molecule in question [19]. As we can see the Ideal Gas Law directly relates pressure and volume, with temperature. This accurately captures the fact that as we heat substances they increase in volume and thus exert more pressure. The Ideal Gas Law was massively over simplified in its most fundamental assumption; namely, that all gases at all temperatures and pressures behave ‘ideally’. This entails that a gas has no intermolecular forces and that the gas particles have no size. In experiments the Ideal Gas Law failed to predict accurate values above one atmosphere, a measurement unit for pressure. An obvious improvement was needed, and came in the form of the Van der Waals equation.

## Van der Waals Equation

The Van der Waals equation was created in 1873 by Johannes van der Waals, and sought to include the two main properties the Ideal Gas Law neglected: Intermolecular forces and the size of particles. As a result the Ideal Gas Law became

$$nRT = (P + \frac{n^2a}{V^2})(V - nb).$$

In the two new terms,  $\frac{n^2a}{V^2}$  and  $nb$ , the constants,  $a$  and  $b$ , represented the attraction between particles and their size respectively. This was an improvement over the Ideal Gas Law, but problems still remained. The value of  $b$  was found non-constant, fluctuating with temperature and pressure [12]. The most significant result stemming from the Van der Waals equation was the Theorem of Corresponding States. In lieu of describing this concept myself, I quote Van der Waals, “Substances behave alike at the same reduced state. Substances at the same reduced states are at corresponding states.”[11]. The essence of the Theorem of Corresponding States is the normalizing of properties of matter. While the concept of normalization is common place to mathematicians, this idea in the physical context at this time was

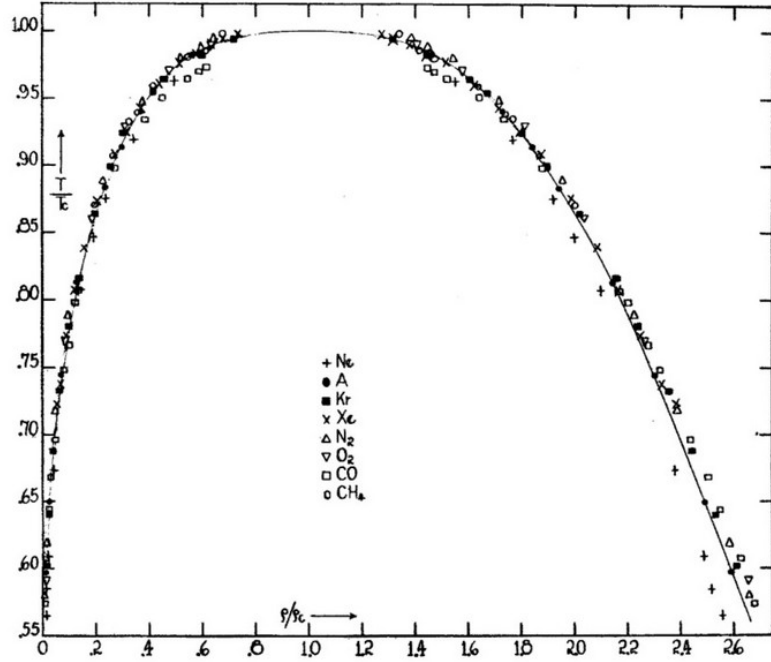


**Figure 2.2:** The x and y axis are  $\bar{P}, \bar{T}$  respectively, [11]

quite novel. Mathematically these reduced states were expressed thusly,

$$\bar{T} = \frac{T}{T_c}, \quad \bar{P} = \frac{P}{P_c}, \quad \bar{V} = \frac{V}{V_c}$$

Quite literally and figuratively the common denominator amongst all of these reduced states is their value at their critical points. The elegant Theorem of Corresponding States was a theorist's dream, but in the physical world, experimental data is required to support theoretical predictions. A particularly convincing example of such evidence is the Guggenheim plot, shown in Figure (2.2). The experimental data supporting the Theorem of Corresponding States is the reason understanding of the physics at and around critical points becomes of such importance. For more information regarding the relevant work of Van der Waals and others, I refer the interested reader to the following sources [11, 19].

Understanding the physics around the critical point requires a new approach. In order to understand what is happening at these all important points, we first need to

pick a property that we suspect will provide some insight. If we return to the water example, we choose to examine the densities of water in its liquid ( $\rho_{liq}$ ) and gaseous phases ( $\rho_{gas}$ ), and consider their differences ( $\Delta\rho = \rho_{liq} - \rho_{gas}$ ). Figure (2.3) plots how this parameter,  $\Delta\rho$ , varies with temperature. As we can see, the difference in densities goes to zero as we approach the critical point, as expected based on the fact that above the critical temperature the differences between the liquid and gas states of water are indistinguishable. This behavior can be encapsulated by the following equation:

$$\Delta\rho = |T_c - T|^{1/2}$$

where  $T < T_c$ . The value  $1/2$  is known as the critical exponent. Its numeric value dictates the behavior of the order parameter,  $\Delta\rho$ , as we approach the critical point. As a result, critical exponents will be largely used to judge the accuracy of any theoretical model as it relates to experimental data. Thus, critical exponents become the main focus of much research in the field of statistical mechanics. Many questions arise, such as: Are there different values for different critical exponents, for different order parameters, or for different models? We shall see a very convenient phenomena will be observed, which will simplify the questions of different critical exponents for different models, much to the relief of physicists. Now let's examine a basic statistical mechanical model, to illustrate some of these concepts.

## 2.2 The Ising Model

The Ising model was developed in 1925 by Ernst Ising at the suggestion of his dissertation advisor. Ising was directed to investigate the phenomena of spontaneous magnetization in magnetic materials. Spontaneous magnetization occurs in certain materials, at specific temperatures, in the presence of some external magnetic field. So what exactly is spontaneous magnetization? Before we can understand that we need to briefly review a little basic physics.

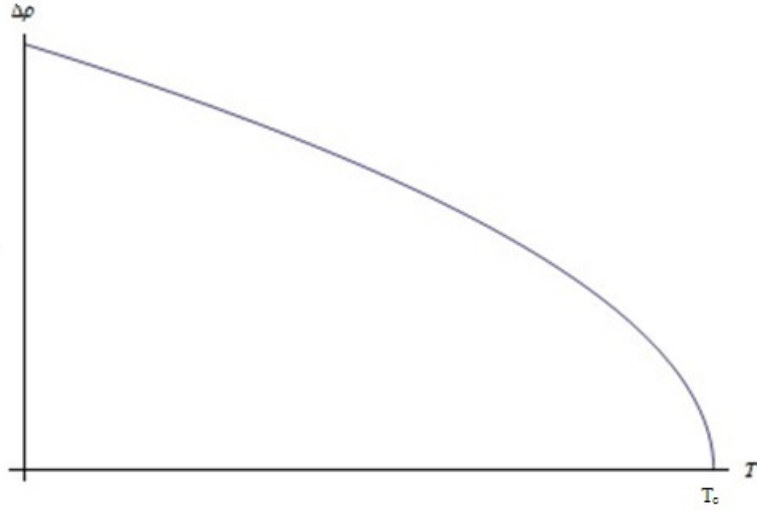


**Figure 2.3:** Notice the exponential decline of  $\Delta\rho$  as  $T \rightarrow T_c$ .

Atoms, the building blocks of all matter, are made up of a nucleus, consisting of positively charged protons and charge-less neutrons, as well as negatively charged electrons which travel in various orbits about the nucleus with some angular velocity. Additionally, every elementary particle has an intrinsic spin, which can be thought of as the spin of a tennis ball rotating about its own axis. (Although not strictly an accurate physical representation, it is sufficient for our intuition.) The concept of intrinsic spin will be of significant physical importance later in the paper. Any charged particle in motion creates its own magnetic field, and thus every individual particle has some small local magnetic field generated by its intrinsic spin. Furthermore, any atom has its own local magnetic field generated by the combination of its constituent charged particles motions, interactions, and inherent spins. Consequently, every atom has what is called a magnetic moment, which is a way of quantifying and capturing the nature of the atomic magnetic field. The two most basic properties are relative strength and direction of the field. As you can imagine the strength and direction of atomic magnetic fields vary widely based on many interacting factors. Using simplified this problem by assuming every atom had an overall spin pointing in either the

‘up’ or ‘down’ direction as illustrated in the one dimensional case by Figure (2.4). The relative orientation of atomic spins will relate to the phenomena of spontaneous magnetization in the Ising model. Now we are ready to define the Ising model.

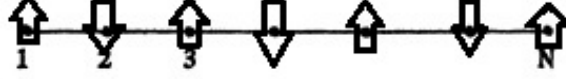


**Figure 2.4:** One dimensional Ising set-up, [5]

Let us recall that the primary objective of the Ising model is to capture the interaction between atoms, as it relates to magnetism. More specifically, the Ising model seeks to discover and describe the conditions under which spontaneous magnetization occurs in a material. A natural place to start is to represent and construct a model for a material. We let our material be represented by a lattice, in dimension  $d$ . This is a finite number  $n$  of equally spaced points, called vertices. Every point is connected to its nearest neighbors exactly once by straight lines called edges. In general the number of edges connected to any given lattice site or vertex is given by  $2d$ . The vertices now represent individual atoms and the edges can be thought of as bonds. See Figure (2.5) for the  $d = 2$  case.

Now that we have our model for the material, it is time to decide how we quantify the properties of the material or system as a whole. This is done with what is called the Hamiltonian, which is a mathematical expression for the energy of a system derived from the relationship between the potential and kinetic energy equations. We can and will, from this point on, think of the Hamiltonian as the overall energy of the system. Before writing the Hamiltonian for the Ising model explicitly, let us recall that the Ising model seeks to capture the interaction between atoms; so in the one dimensional case for example, given any atom we wish to know how it interacts with its neighboring left and right atoms. This interaction, in the context of magnetism, is the interaction of atomic spins. Let’s make some of these qualitative notions concrete with the explicit expression of atomic interaction and hence overall energy  $H$  (the Hamiltonian) of the system for the Ising model.

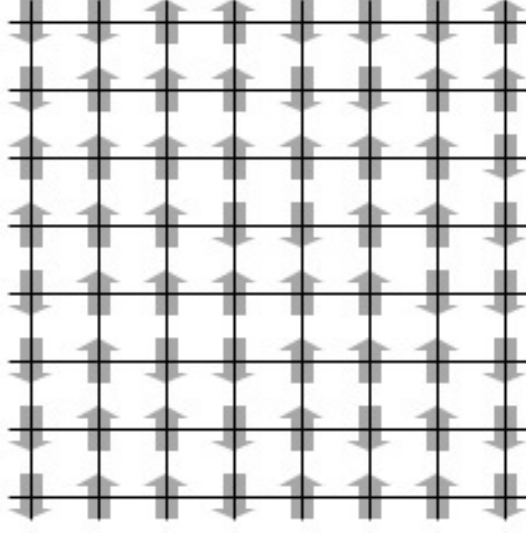


**Figure 2.5:** Two dimensional Ising model set-up, courtesy Alexander Papageorge.

Let  $\sigma = \{1, 2, \dots, n\}$  be the vertices of our  $d$ -dimensional lattice and let  $\sigma = \{\sigma_1, \dots, \sigma_n\}$  with  $\sigma_i = +1$  represent the ‘spin up’ and  $\sigma = -1$  ‘spin down’, for,  $i \in \{1, \dots, n\}$ . Then the total energy of the system  $H$  can be represented by

$$H(\sigma) = -J \sum_{\langle i, j \rangle} \sigma_i \sigma_j \quad (2.1)$$

where  $J > 0$  is known as the coupling constant, and the notation  $\langle i, j \rangle$  means to sum over all nearest neighbor vertex pairs. There is a symmetry about the model, so  $H(\sigma) = -H(\sigma)$ . In other words the spin values are symmetric: if we multiply the model by -1, all the spins flip and become their inverses. Here  $H$  is given as a function of  $\sigma$  because the value of  $H$  depends upon the various distributions of +1’s and -1’s ‘spins’. Also we see that the interaction between atoms is given by the product of values that the vertices take. So if the spins of one neighboring pair of atoms point in the same direction, i.e.  $\sigma_i = \sigma_j = +1$  or  $\sigma_i = \sigma_j = -1$ , then their interaction, the product  $\sigma_i \sigma_j$  always equals 1. We also see, due to the negative sign in front of the sum and the fact that  $J > 0$  the neighboring spins have a preference to align, in physical terms. This is what is known as ferromagnetism. Let’s consider a quick

example in 1-dimension with  $n = 3$ . Suppose  $\sigma_1 = \sigma_3 = +1$  and  $\sigma_2 = -1$ . Then,

$$\begin{aligned}
 H(\sigma) &= -J \sum_{\langle i,j \rangle} \sigma_i \sigma_j \\
 &= -J[\sigma_1 \sigma_2 + \sigma_2 \sigma_3] \\
 &= -J[(1)(-1) + (-1)(1)] \\
 &= 2J
 \end{aligned}$$

Equation (2.1) is the basic Ising model; however, it is not the complete Ising model, which takes into account an external magnetic field. As with all magnetic fields, there is a specific direction associated with the external magnetic field. For simplicity's sake, Ising again chose the direction to either be up or down. The effect of the external magnetic field depends on several factors. In addition to its direction, the strength of the external field and the temperature of the material are important parameters. The reason temperature is related to the magnetism of a material is due to the two main types of magnetism: ferromagnetism and paramagnetism. The point which separates these two types of magnetism is the Currie point, and it is akin to the boiling point of liquid. A material's transition from ferromagnetic to paramagnetic is in fact a phase transition: a material is ferromagnetic below its Currie temperature, where all atomic spins align in the same direction, and remains magnetic even in the absence of an external magnetic field. The everyday magnetics on our refrigerator are examples of ferromagnetic materials. In contrast, a material can only be paramagnetic above its Currie temperature. Paramagnetism is characterized by random atomic spin directions. Additionally, when a material is paramagnetic the randomized spins **will align** in the presence of an external magnetic field. The order parameters associated with ferromagnetism and paramagnetism are average magnetization ( $M$ ) and magnetic susceptibility ( $\chi$ ) respectively. See Figures (2.6, 2.7).

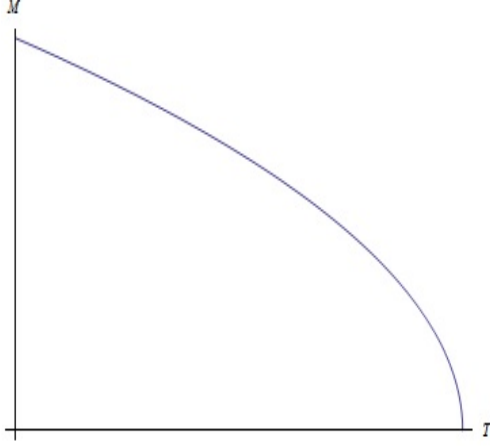


**Figure 2.6:** Average magnetization order parameter

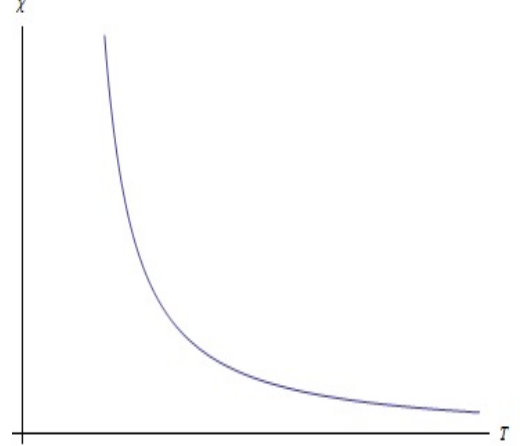


**Figure 2.7:** Magnetic susceptibility order parameter

This makes sense intuitively, since at temperatures above the Currie point, where a material becomes paramagnetic, we are quite literally measuring how susceptible its random spins are to the influence of an external magnetic field. We quantify this behavior in a similar fashion to the order parameters already encountered before. Below the Currie point, i.e. for  $T < T_c$  the average magnetization ( $M$ ) is given by

$$M \sim |T_c - T|^\alpha$$

Similarly, when we are above the Currie point, i.e.  $T_c < T$  the magnetic susceptibility ( $\chi$ ) is given by,

$$\chi \sim \frac{1}{|T - T_c|^\gamma}$$

Notice the critical exponents  $\alpha$  and  $\gamma$  play the same important role as they did before. Figure (2.8) graphs both of these parameters, with predicted values of the critical exponents. We refer the reader to the following sources for more information on how to explicitly calculate critical exponents [4, 5, 8]. We can see as temperature continues to increase, random thermal fluctuations begin to overpower the influence of the external magnetic field and dominate the system. The goal of the Ising model is to



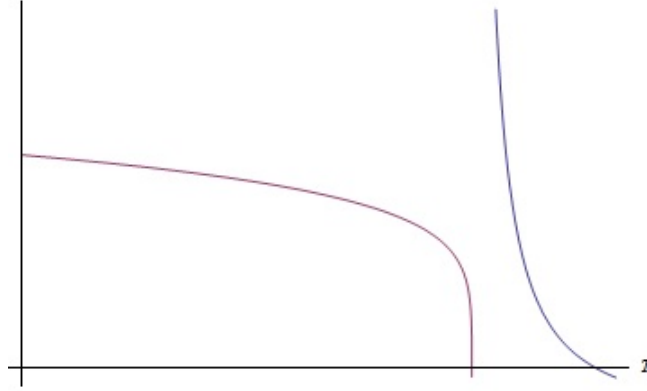
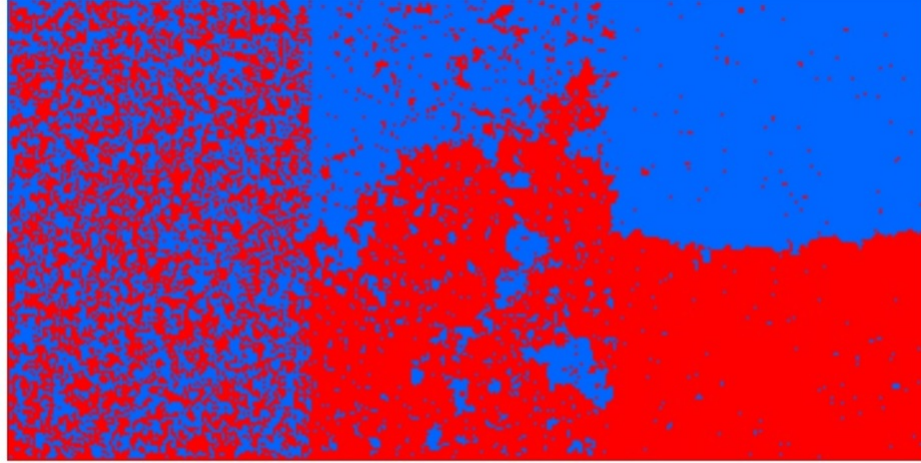


**Figure 2.8:** Notice the mutual asymptotic behavior at the critical temperature.

model gain a greater understanding of the interplay and relationships between these relevant parameters.

As both of these order parameters indicate, magnetic properties are a function of temperature, and as a consequence the distribution of spins across the Ising model also varies with temperature. In other words parts of the model may have up spins, others down. In the absence of an external magnetic field, the distribution of these spins across the model is a function of temperature only. At temperatures above the Currie point, thermal fluctuations overpower any magnetic properties the model may have, hence the small clusters of aligned spins as the  $T_c < T$  portion of Figure (2.9) illustrates. As temperature decreases, the first point at which magnetic properties can begin to overpower thermal fluctuations is critical temperature. At this temperature the model develops more equally sized clusters of up and down spins, as shown at  $T=T_c$  in Figure (2.9). The boundary which divides the two largest continuous clusters is known as the *domain wall*. The domination of the magnetic properties continues as temperatures decrease, changing the direction of the remaining pockets of spins whose directions are opposite that of the larger cluster surrounding it. This continues until an equilibrium is reached, with an equal distribution of up and down spins across the model, as indicated by Figure (2.9) at  $T < T_c$ .



$T_c < T$

$T_c = T$

$T < T_c$

**Figure 2.9:** The Ising model with Dobrushin boundary conditions, and no external magnetic field, at various temperatures, notice the appearance of the red-blue interface known as the domain wall at  $T = T_c$  [9].

We now introduce the complete Ising model,

$$H(\sigma) = -J \sum_{\langle i,j \rangle} \sigma_i \sigma_j - h \sum_i \sigma_i \quad (2.2)$$

where  $h$  is a parameter representing the strength of the external magnetic field. The second sum represents the external magnetic field acting on each lattice site equally. Note the similarity to our previous version of the Ising model; in fact, this model reduces to (2.1) when  $h = 0$ .

Now that we have a complete model capturing basic atomic interaction in the presence of an external magnetic field, we need to discuss what we do with the Hamiltonian in order to derive more useful information from this model. The way we do this is by utilizing a cornerstone of Statistical Mechanics, the partition function. The partition function is an entirely mathematical tool formed by taking the exponential of the Hamiltonian and then summing over all the possible distributions of  $\pm 1$ 's spins. To be clear, if we consider as before the case of  $n = 3$  then we have  $2^3$  sets to sum over. Examples of such sets are  $\sigma^1 = \{1, 1, 1\}$  or  $\sigma^2 = \{1, 1, -1\}$ .

Since each  $\sigma_i$  can take one of two values namely, +1 or -1, and because the number of vertices is 3, we see there are  $2^3 = 8$  possible sets to sum over. In general, we will be summing over  $2^n$  sets. For simplicity and introductory purposes we can introduce the partition function over the Hamiltonian with no external magnetic field. Then we have the partition function defined as follows,

$$Z = \sum_{\{\sigma^i\}} e^{-\beta H(\sigma^i)} \quad (2.3)$$

where  $\beta$  is a parameter used to cancel whatever units the Hamiltonian may have. Typically,  $\beta = \frac{1}{kT}$  where  $T$  represents temperature and  $k$  is Boltzmann's constant, and this is how we will think of  $\beta$  throughout the rest of this paper. The partition function allows us to obtain a weighted value representing the probability that we will find our system in a particular state:

$$Prob(\sigma^k) = \frac{e^{-\beta H(\sigma^k)}}{Z} \quad (2.4)$$

Here we can see  $Z$  as the normalizing denominator since by definition it includes all of the possible states the model may obtain.

The most basic Ising model did not exhibit a phase transition in one dimension, and its oversimplification of atomic interactions needed to be rectified. Physicists introduced mean field theory to the Ising model to solve this inadequacy. In actuality, the interaction between atomic magnetic fields are far more complex than the original Ising model assumed. Atoms do not interact one at a time with each other, but rather are constantly all acting on each other simultaneously. As a analogy consider a network of buckets full of water, all connected to each other by a series of hollow tubes allowing water to flow between the buckets. Each bucket is either full of hot or cold water, mimicking the spin up or spin down of the Ising model. As the Ising model is originally defined, the water in the center bucket interacts only with one neighboring bucket at a time; meaning that, at any given time only two buckets are

exchanging water. We want the water in all the buckets to be mixing with all the other buckets simultaneously. In other words, we want all the water, from all the buckets, to freely flow between the buckets all the time. As the entire amount of water mixes, the hot and cold water combine, reaching an average or mean temperature over the network of buckets. This is exactly the atomic interaction we want to achieve and it is known as mean field theory. In the context of the Ising model, the necessary adjustment to achieve the mean field theory effect amounts to a small mathematical change illustrated below.

The first thing we need to do to capture this average or mean behavior over a set of lattice sites, is to first rewrite the atomic interaction. As it stands now the atomic interaction is the product  $\sigma_i\sigma_j$ . So we rewrite it as the following,

$$\begin{aligned}\sigma_i\sigma_j &= [(\sigma_i - m) + m][(\sigma_j - m) + m] \\ &= (\sigma_i - m)(\sigma_j - m) + (\sigma_i - m)m + (\sigma_j - m)m + m^2\end{aligned}$$

where  $m$  is the average spin. So we are considering the difference between any given spin and the mean spin of over all its neighbors. We are also assuming that the spin of any given lattice site deviates only slightly from the average spin of all its neighbors, so  $(\sigma_i - m) \approx 0$  and  $(\sigma_j - m) \approx 0$ . So when we sum over all pairs in calculating the new Hamiltonian we can neglect the  $(\sigma_i - m)(\sigma_j - m)$  term. Thus the Hamiltonian for the mean field theory approximation can be formulated as,

$$\begin{aligned}H &= -J \sum_{\langle i,j \rangle} [m(\sigma_i + \sigma_j) - m^2] - h \sum_i \sigma_i \\ &= \frac{1}{2} J m^2 n d - (J m d + h) \sum_i \sigma_i\end{aligned}\tag{2.5}$$

where the factor  $nd/2$  is the number of nearest neighbor pairs since  $d$  is the dimension and  $n$  is the number of edges connecting the vertices. This equation is a modification of equation (2.2) because we were able to neglect the  $(\sigma_i - m)(\sigma_j - m)$  term, so they

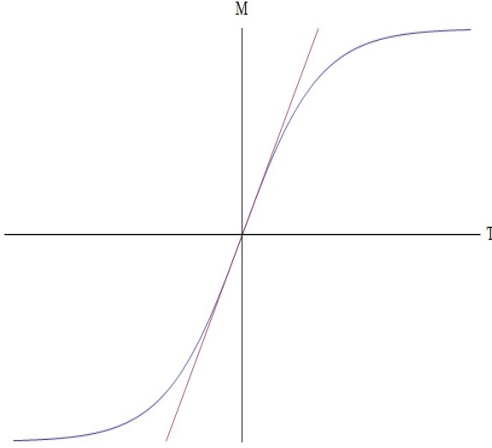


**Figure 2.10:** High temperature

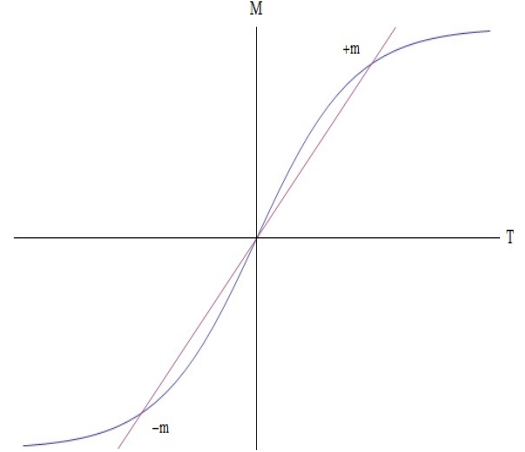


**Figure 2.11:** Low temperature

are not equivalent equations. The interactions for this version of the Ising model have been changed in that a spin is now effected by the mean spin of its neighbors. This local magnetic field can now contribute to the force of the external magnetic field, as indicated by the  $(Jmd + h)$  term. The term  $(Jmd + h)$  is the new external magnetic field and we will denote it as  $h_m = Jmd + h$ . So what effect does this new term have on the overall system, and what is the effect when there is no external magnetic field versus when there is one? Well lets compare the equations when  $h = 0$  and when  $h = Jmd$ .

When  $h = 0$  then  $h_m = Jmd$ . So our the partition function for the mean field approximation can be written as,

$$\begin{aligned} Z &= e^{-\frac{1}{2}\beta m^2 Jnd} (e^{-\beta h_m} + e^{\beta h_m})^n \\ &= e^{-\frac{1}{2}\beta m^2 Jnd} 2^n \cosh^n(\beta h_m) . \end{aligned}$$

Note that in the term  $h_m = Jmd + h$ , the values  $J, h$  and  $d$  are fixed. Thus  $h_m$  depends on the mean value  $m$ . But what is the value of  $m$ ? We can solve for  $m$  using the expression of our partition function  $Z$ , and we find that

$$m = \tanh(\beta h + 2\beta Jdm).$$

To investigate the value of  $m$  further let us consider the case when  $h = 0$ , then  $h_m = Jmd$ , thus  $m = \tanh(\beta Jdm)$ . Recall  $\beta = 1/kT$  so we are able to relate the value of  $m$  with temperature based on the above equation. Figures (2.10, 2.11) illustrate the relationship between the values of  $m$  and the temperature  $T$ . Figure (2.10) can be interpreted as a system at high temperatures, hence the lack of any average magnetization. Figure (2.11) depicts the case where  $Jnd > 1$ , where we have three distinct solutions:  $+m$ ,  $-m$  and  $0$ . The solutions represent atomic interactions overcoming the effects of temperature and thus yielding a non-zero mean magnetization value. The temperature dividing these two cases is known as the critical temperature and is given by  $kT_c = J2d$ .

Next, let's consider the effect on the system when  $h \neq 0$ . Since the term  $\tanh(\beta h + 2\beta Jdm)$  now has the  $\beta h$  term we see a left or rightward shift of the entire graph depending on the sign  $h$  takes. See Figure (2.12).

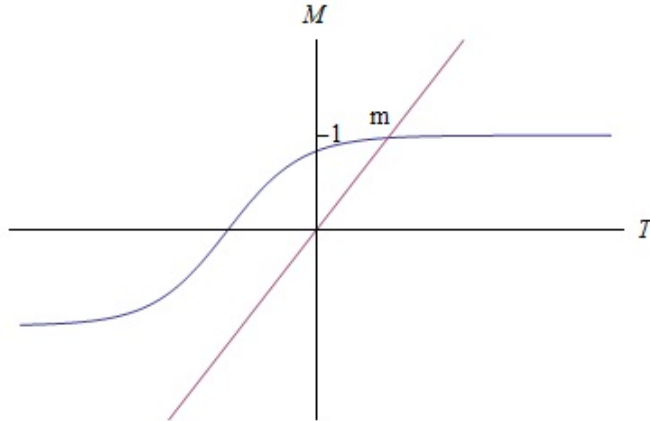


**Figure 2.12:**  $h > 0$  so we see positive  $m$  is the only solution.

Now that we have a good idea of the physics underlying the Ising model and how it works, we can ask ourselves the most important question of all: How well does the model work? One way to address this question is to use the model to predict critical exponents and then compare them to experimental data. Sadly, the Ising models predicted critical exponents do not agree with experimental data. The table below

provides the theoretical and experimental values of critical exponents for both the Ising model and the more familiar liquid-gas phase transition.

**Table 2.1:** Comparison of Ising model data [16]

Variable	parameter	predicted	experimental
$\chi$	mag susp	1	1.2
$M$	avg mag	1/2	.32
$\Delta\rho$	$\Delta$ density	1/2	.32
$\kappa$	compressibility	1	1.2

The most fascinating fact about this table is the exact same results for two completely different physical processes. The fact that the Ising model provided the same results, albeit incorrect, for liquid-gas transition as it did for magnetic phase transitions greatly simplified the physicist's task. Instead of creating different models with different order parameters for various types of phase transitions there seemed to be a *universality* to the underlying physics, hinting at the possibility of creating one general model which could describe many if not all processes in statistical mechanics. This hope brought many mathematicians to the realm of statistical mechanics, as they attempted to construct or apply the appropriate mathematical theory that would yield an elegant general model.

## 2.3 Advanced Physics

### The Renormalization Group

In the previous sections we discussed some basic physics and one of the most prominent statistical mechanics models, the Ising model. In that discussion we saw how the all-important critical exponents serve as our gauge of validity for a particular model. We also saw that even with the addition of mean field theory, the Ising model still did not quite agree with experimental data. The next step in our journey is to discuss the physicists proposed solution to fix the Ising model.

The failure of both the basic and improved Ising models is the inability to accurately capture the atomic fluctuations within a material at or near its critical value, as Table (2.1) illustrated numerically. In order to rectify these shortcomings the physics community essentially created two new mathematical tools: the renormalization group and conformal field theory. Without going into much detail describing either one of these advanced concepts, I would like to take a moment to discuss the ideas behind them, illustrate what they achieve, and mention their shortcomings. Understanding these ideas is the key to realizing the need for a more rigorous mathematical formalism and thus directly motivating the development of Schramm-Loewner Evolution.

As the above example illustrated, the basic and improved Ising models fail to take into account the fluctuations of atomic interaction near critical values. Intuitively, these models are too rough of an approximation to capture the fine, complex interactions happening on the smallest scales at critical values; interactions which in turn, dictate the macroscopic behavior of the model. This is the problem that the renormalization group intended to solve. The renormalization group is a mathematical method used to effectively calculate and recalculate various model parameters, as the scale on which these parameters are observed changes. As an analogy, if one observes, from the height of 100 ft above some track, a car moving at a constant speed of 100 mi/hr around said track, one could accurately confirm its speed given information like how big the track is, lap times, etc. If we increase our observational height to 10,000 ft we cannot see the car or the track well enough to confirm the car's speed. If we could zoom in enough to replicate the 100 ft perspective we could then confirm the speed of the car. The renormalization group plays the role of the zooming in action needed to reacquire the 100 ft perspective. Just as the analogy seeks to verify the velocity of the car, in reality an experimenter can try to measure the velocity of a particle. One can renormalize many physically observable parameters of a system. Examples of this include, velocity, momentum, spin, and position, of a particle in a thermodynamic system. To restate, renormalizing



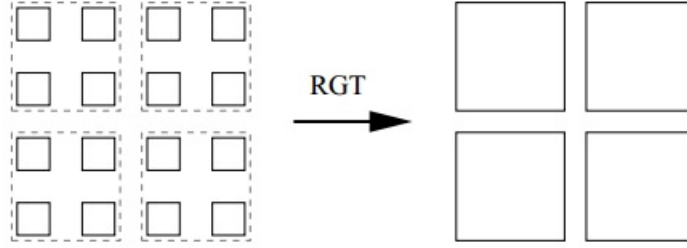


**Figure 2.13:** Coarse-graining process. image courtesy Andreas Dengerhard and Javier Rodriguez-Laguna

a parameter of a model ensures the numerical value of that parameter stays consistent with respect to the original scaling, once we have changed the observational scale. Examples of this scaling problem are abundant across the various realms of physics. Perhaps most notably is the Theory of Relativity’s inability to accurately describing the universe on the quantum scale, although succeeding brilliantly on cosmic scales. Conversely, quantum mechanics flourishes on the quantum scale but falters on any scale larger than the microscopic.

The main procedure for renormalizing a system is called coarse-graining. The process for the Ising model proceeds as follows. Given a finite lattice with some distribution of spins on it, we first divide the lattice into blocks of equal size. Next, assign the entire block the spin that occurs most frequently within it. The belief being that if we replace the many spins within the blocks across the entire model with only one spin per block, we are effectively changing the observation scale appropriately for the model. See Figure (2.13) for illustration. If this process was repeated sufficiently many times, on the Ising model for example, the belief was that at the critical temperature, as we refined our lattice over and over, the model would ‘converge’ to a continuous, and thus most realistic, version of the Ising model. This would also allow the Ising model to then fall within the scope of a quantum field theory, since the spaces between our atoms would have gone to zero, we would have a continuous field of atoms as opposed to a discrete lattice of atoms. This limiting process is what physicists call the continuum limit and what mathematicians call the scaling limit, which I will

discuss below. But first note, if we can make a model such as Ising's converge to a continuous space at criticality, what is to stop us from doing the same for any lattice model? This is the concept of universality, eluded to in Table (2.1), and in this new context states that as long as models belong to the same so-called renormalization space then the scaling or continuum limit should always be the same. As a result, the scaling limit must be invariant under rotations and translations, and it was further suggested that since the scaling limit is now a quantum field theory, it should or may be conformally invariant. [8] This triggered an onslaught of research in the subject of conformal field theory, as both mathematicians and physicists hoped to confirm these new conjectures. See [1, 15] for more details regarding the renormalization group.

## Conformal Field Theory

While the mathematical mechanics of the renormalization group is daunting, I do want to briefly mention one of its chief components, conformal field theory. Conformal field theory is a subset of quantum field theory, and as such, the objects it examines are fundamental particles and other phenomena on the quantum scale. Because these particles tend to possess some inherent symmetry, the mathematical discipline of algebra, as one might expect, is the natural tool used for their analysis. In particular, the symmetry and interactions of these quantum objects is such that they may be represented as fields. This allows all of the tools of group and field theory to be fully utilized in their study. Conformal fields are distinguished from ordinary fields in that their symmetry groups are invariant under a conformal mapping, hence the name conformal field theory. Conformal field theory has been extensively researched and is the machinery of choice when analyzing behaviors of two dimensional lattice models at criticality. The predictions of conformal field theory, including the all-important values of critical exponents, have provided the closest agreement with experimental data to date. While conformal field theory itself is mathematically justified, many of the physical and mathematical presumptions which originally inspired the use of

conformal field theory were not fully justified. For as much success as conformal field theory was enjoying, there were still some very basic cases, namely that of the percolation process model, where conformal field theory failed to provide complete or convincing answers. For more details concerning conformal field theory see [10].

## Shortcomings

The problem with the renormalization group and conformal field theory approaches stem from a very subtle difference between the continuum and scaling limits as defined by the physics and mathematical communities respectively. Physicists often need to move impossibly difficult problems in a continuous space, which is where they occur in nature, to a discrete space where the problem becomes more manageable. A lattice is an example of this discretization of continuous space. In order to recapture the *continuous space*, the lattice spacing is taken to zero, hence the name *continuum limit*. Mathematicians refer to this as the *scaling limit*, because it refers to the size of the lattice *scale* being taken to zero. And as described in the renormalization group section, it is in the limit, at criticality, which gives rise to the conformally invariant object. But it is in the nature of the object in question where the subtle but important distinction between these two definitions occurs. The continuum limit refers to recapturing the behavior of the entire discrete model in continuous space. This is at odds with the mathematical notion of the scaling limit because the scaling limit depends on a specific object defined on the model. For mathematicians, “the meaning of the scaling limit depends on the object we wish to study (interfaces, size of clusters, crossing, etc.),” rather than the limit of an entire model. [8] The differences between these two definitions is further compounded by the assumption physicists assert regarding the existence of such a limit, whereas mathematicians before considering a limiting object, must first be able to prove its existence. This is a detail that is often glazed over by both disciplines and one which poses a fundamental obstacle in connecting the numerical predictions of physicists to the

rigorous mathematical justifications necessary to make such predictions. Schramm-Loewner Evolution addresses this fundamental problem and provides the rigorous mathematical foundation necessary to realize this connection. For the interested reader, in addition to the sources I have already provided I highly recommend David Tong's home page from the University of Cambridge for any and all interests pertaining to physics.

## **A Quick Recap**

We have introduced a large amount of physics thus far, and it can be easy to lose sight of the bigger picture. Figure (2.13) provides you with a basic overview and progression of the essential physical ideas we have discussed. We set out to investigate the mechanisms and properties of phase transitions of matter. This led us to Van der Waals Equation, which admitted critical exponents. Fundamentally incorrect assumptions about the constants in the model and disagreement between experimental theoretical data highlighted the need for a new approach. This came in the form of conformal field theory, which drastically increased the accuracy of critical exponents and made many strong predictions about model behavior supported by numerical simulations. As we shall see at the end of chapter 3, SLE will rigorously confirm these numerical simulations, and provided insight to many other statistical mechanical models.

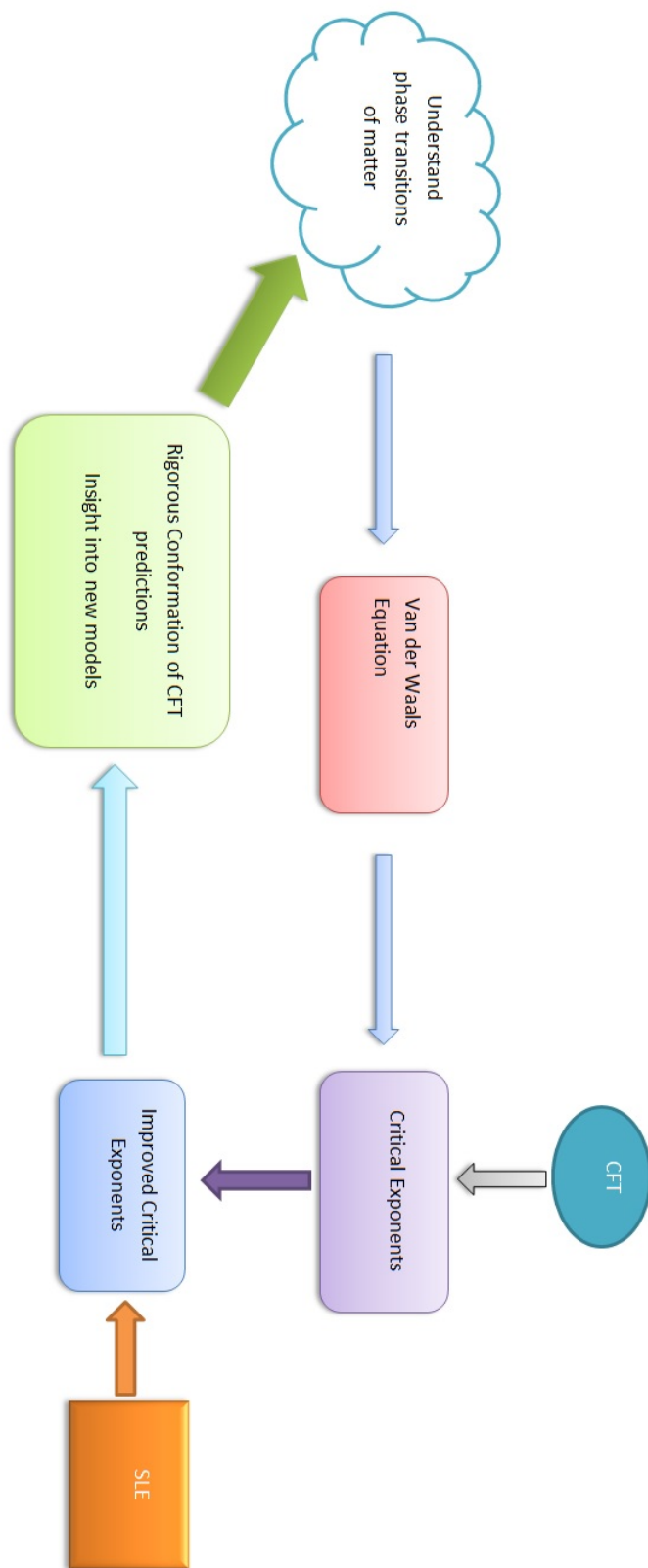


**Figure 2.14:** Highlights of our journey thus far.

# Chapter 3

## Introduction to Schramm-Loewner Evolution Concepts

### 3.1 Schramm-Loewner Evolution

Statistical mechanics and condensed matter physics had just undergone a revolution. Substantial progress on the simple yet vexing question of phase transitions in lattice models had recently been made with the advent and application of two new elaborate and mathematically dense methods: the renormalization group and conformal field theory. While the physics community celebrated and supported their hypotheses with compelling numerical simulations, mathematicians were still grappling with some of the underlying assumptions their physicist brethren had assumed to be true, without rigorous proof. What mathematicians wanted was an organic and rigorous process which could duplicate the same successes and insights the renormalization group and conformal field theory had generated. The Schramm-Loewner Evolution, as it would come to be called, was created to accomplish exactly that.

The intent of Schramm-Loewner Evolution (SLE) is twofold: To solve the physical problems posed by physicists and to satisfy the mathematicians need for rigor and proof. As previously mentioned, in order to solve the physicist

problems we need a continuous, conformally invariant object. But we also require a mathematically rigorous process which satisfies these requirements. We begin first with an introduction to the relevant concepts from probability.

## Necessary Probability

The first and most basic concept is that of a *simple random walk*. In the one dimensional case, consider the integers on a number line. After picking an arbitrary starting point, we can then only move the distance of one integer at a time. For example, if we start at 0, we can only move to -1 or +1. Whether we move to -1 or +1 is dictated by probability, in this case an equal 50-50 chance of moving to either number. Supposing we move to +1, then the same probability applies for the next step, a 50% chance of moving to either +2 or back to 0. This process repeats itself any number of times, and the resulting movement along the number line is known as a random walk. A simple random walk can be defined in any dimension. If we want a random walk on a lattice, we can think of it in the following way: Imagine you start at any vertex on the lattice at time zero, and you can only move one vertex at every time interval. In the case of a two dimensional square lattice, there is an equal 25% chance of moving to the vertex on your left, right, straight ahead, or behind. This process repeats just as in the one dimensional case, and the path traversed is known as a simple random walk. See Figure (3.1). A slight variation of the simple random walk is the *loop erased random walk* (LERW). This is just a simple random walk with the additional condition that any loops created while performing the random walk are eliminated. See Figure (3.2).

In the 1950's Donsker proved that as the step size goes to zero, a simple random walk, when appropriately scaled, converges to the well known process called *Brownian motion* [7]. Brownian motion was originally created to study the random movements of gas particles. The path Brownian motion creates is everywhere continuous but nowhere differentiable in the usual sense. (It is differentiable using a stochastically

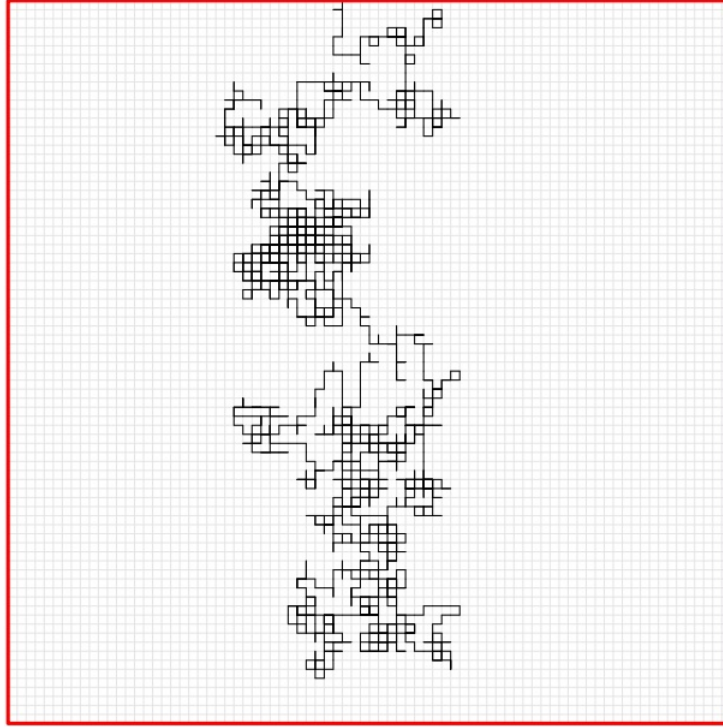


**Figure 3.1:** An example of a 2-d random walk on a square lattice, courtesy Tom Alberts.

developed form of calculus known as Itô calculus.) Schramm was trying to understand the same problem for other random walks, such as LERW. Intuitively, this is a simple idea. Figure (3.2) is a LERW on a square lattice, but what happens to the curves as we shrink the size of the squares? Does this discrete LERW on a square lattice converge to a continuous curve in a continuous space as we take the square size to zero? This is the notion of a scaling limit Schramm began to investigate. In addition to showing the scaling limit existed, he also wanted to prove that the limit is conformally invariant, a property held by Brownian motion. This was desirable because as predicted by conformal field theory, continuous and conformally invariant curves were qualities associated with two dimensional lattice models at criticality. But we still need to tie in the physical models explicitly, and relate them to the mathematics, in order to achieve that we need one additional concept from probability, the *martingale*.



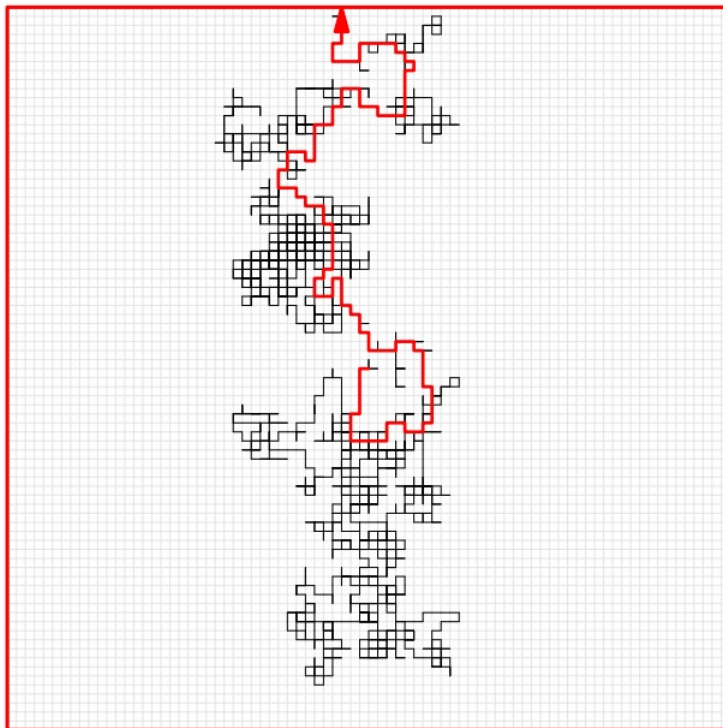


**Figure 3.2:** An example of a 2-d LERW, courtesy Tom Alberts.

A martingale is a random process where the future depends only on the current state, and not on the past. An example of a martingale is a simple random walk. As previously described, the next step in a random walk is not affected by past events, and all future steps have an equal probability of occurring. So we see the properties of a martingale occurring in the context of a simple random walk. It has also been shown that Brownian motion is a martingale in [13]. In the SLE context, the mathematical representation of a physical *observable* may be represented as a martingale. Intuitively speaking an observable is any measureable quantity of a physical system, for example position, momentum, or spin. Mathematically speaking, the observation takes place in the realm of quantum theory, so a particular continuous linear operator is assigned to each observable quantity. For example, if you wish to observe momentum, a specific continuous linear operator, usually in the form of a matrix, will be associated with momentum. This operator acts on the states of the system which are represented by

vectors. The representation of an observable as a martingale is how SLE knits itself into the physical models of statistical mechanics.

Now we need a way to connect all of these ideas together, concisely and rigorously. We need a way to ensure our discrete random walk converges to a continuous curve in a continuous space of physical relevance. The mechanism which would provide all of this was the Loewner Equation.

## The Loewner Equation

We start this section with an introduction to the basic Loewner before discussing Schramm's unique utilization of it. The Loewner equation is defined as the following differential equation.

**Definition.** Denote  $\mathbb{H} = \{z \in \mathbb{C} : \text{Im}(z) > 0\}$  as the upper half-plane. Let  $z \in \mathbb{H}$  and  $\lambda(t)$  be a continuous real valued function for  $t \in [0, T]$ . Then the Loewner equation is the initial value problem,

$$\frac{\partial}{\partial t}g(z, t) = \frac{2}{g(z, t) - \lambda(t)} \quad , \quad g(z, 0) = z \quad . \quad (3.1)$$

The existence and uniqueness theorem for differential equations guarantees that for every  $z \in \mathbb{H}$  there exists a unique solution to the Loewner Equation on some time interval  $[0, t_0)$ . There are two sets of interest which result from (3.1). The first relates to the set of times for which the solution to (3.1) makes sense. We define this set in the following way: Let  $T_z = \sup\{t_0 \in [0, T] : g(z, t) \text{ exists on } [0, t_0)\}$ . This defines our set of valid times for a fixed  $z$ . The second set we need to consider is the set of valid points in  $\mathbb{H}$  such that  $g(z, t) \neq \lambda(t)$ . For a fixed  $t \in [0, T]$  define  $G_t = \{z \in \mathbb{H} : t < T_z\}$ , and define  $K_t = \mathbb{H} \setminus G_t$ , which is called the *hull*. It is a classic result that the solution to (3.1) is a conformal mapping from  $G_t$  onto  $\mathbb{H}$ .

Starting with  $\lambda(t)$ , which is also known as the driving function, we know that through the mechanics of (3.1) a simply connected domain in the form of  $G_t$  and the related hull,  $K_t$  will be produced. Additionally, the solution to (3.1) yields a

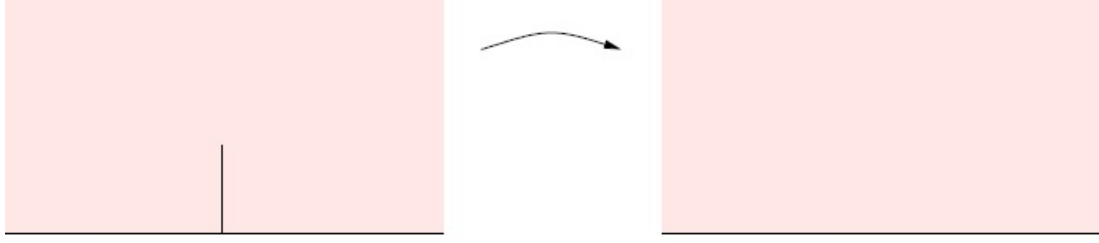


**Figure 3.3:** An example of the Loewner trace when  $\lambda(t) = 0$  and the corresponding mapping onto  $\mathbb{H}$ , courtesy Joan Lind.

conformal map,  $g_t(z) : G_t \rightarrow \mathbb{H}$ . Properties of  $\lambda(t)$  affect the geometry of  $K_t$ . In some cases  $K_t = \gamma(0, t]$  for a simple curve  $\gamma$  in  $\mathbb{H}$  with  $\gamma(0) \in \mathbb{R}$ . In a slightly more complicated situation,  $K_t$  may be determined by a non-simple curve  $\gamma$  in  $\mathbb{H}$  that is allowed to touch back on itself or on the real line, but not cross over itself. Then  $K_t$  is the union of the curve  $\gamma(0, t]$  with all the bounded components of  $\mathbb{H} \setminus \gamma(0, t]$ . In both cases, the curve, called the trace, completely determines the hull  $K_t$ . When a hull is defined by a trace curve  $\gamma$ , then  $\lambda(t) = g_t(\gamma(t))$ , or in other words, the driving function is image of the tip of the curve under the conformal map  $g_t$ . As we can see, the choice of  $\lambda(t)$  underpins everything in the Loewner Equation, including the conformal mapping.

Now that we understand the basic properties of the Loewner Equation let's illustrate them with a simple example.

**Example 1.** Let the driving function  $\lambda(t) = 0$  for all  $t \in [0, T]$ . Then (3.1) reduces very nicely to

$$\frac{\partial}{\partial t} g(z, t) = \frac{2}{g(z, t)}$$

We can solve this simply by separation of variable as follows:

$$\begin{aligned}
g(z, t) \frac{\partial}{\partial t} g(z, t) &= 2 \\
\int \left( g(z, t) \frac{\partial}{\partial t} g(z, t) \right) dt &= \int 2 dt \\
\frac{1}{2} g(z, t)^2 &= 2t + C \\
g(z, t) &= \sqrt{4t + 2C}
\end{aligned}$$

To find  $C$ , we use the initial condition:  $g(z, 0) = \sqrt{2C} = z$ . Thus,

$$g(z, t) = \sqrt{4t + z^2}$$

In example 1, the conformal map generated by the Loewner equation is  $g(z, t) = \sqrt{4t + z^2}$ , which is a conformal map from  $\mathbb{H}$  with a vertical slit removed onto  $\mathbb{H}$ , as shown in Figure (3.3). In this example, the hull is the vertical slit  $\{iy : 0 \leq y \leq 2\sqrt{t}\}$ , and the trace is the curve  $\gamma(t) = 2i\sqrt{t}$ . We see that  $g(z, t)$  takes the tip of the trace and maps it to 0 since  $g_t(2i\sqrt{t}) = \sqrt{4t - 4t} = 0 = \lambda(t)$ .

Now that we have a grasp on the Loewner Equation we are ready to give a definition of SLE.

**Definition.**  $\text{SLE}(\kappa)$  is the random trace curve generated by the Loewner Equation when  $\lambda(t) = \sqrt{\kappa}B_t$ , where  $B_t$  is Brownian motion.

The stochastic nature of Brownian motion enabled the Loewner Equation to produce a random families of curves, which were by definition continuous and conformally invariant. In the case of SLE, the parameter  $\kappa$  dictates the properties of the trace and hence these randomly produced curves. It has been shown in [17] that there is a unique and continuous path  $\gamma : [0, \infty) \rightarrow \mathbb{H}$  such that the hull is the union of  $\gamma[0, t]$  and the connected components of  $\mathbb{H} \setminus \gamma[0, t]$ . The evolution of  $\gamma(t)$  along with its shape and properties when  $\lambda(t) = \sqrt{\kappa}B_t$  is the defining aspect of SLE. Figures (3.4, 3.5) gives some examples of such curves when  $\kappa = 2$  and

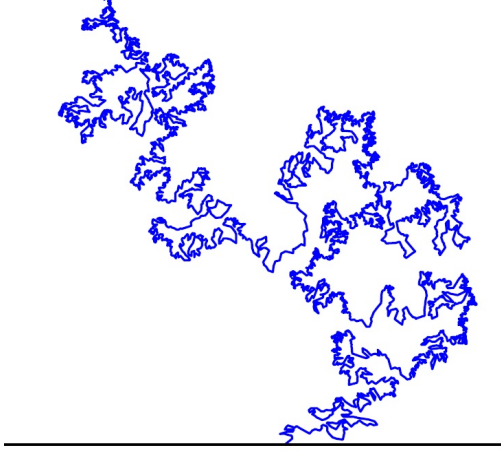


**Figure 3.4:** The curve  $\gamma(t)$  when  $\lambda(t) = \sqrt{6}B_t$ , courtesy Joan Lind

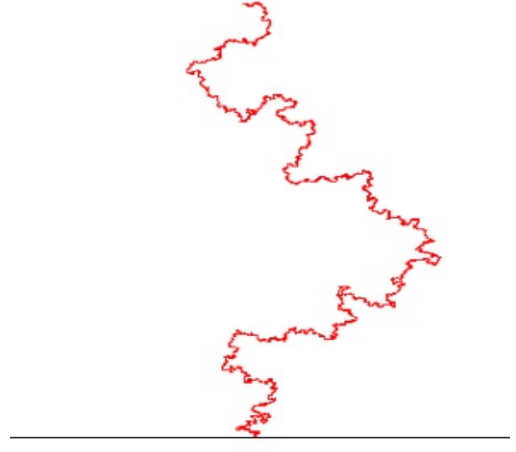


**Figure 3.5:** The curve  $\gamma(t)$  when  $\lambda(t) = \sqrt{2}B_t$ , courtesy Tom Alberts

$\kappa = 6$ . These curves were the candidates for the scaling limits mathematicians sought. In order to identify the appropriate SLE curve for a particular model, say the domain wall in the Ising model or the LERW for example, mathematicians needed a way to use features of the model to determine a particular value of  $\kappa$ . This was accomplished by finding a physical observable connected with the model at hand that could be mathematically represented as a martingale. Then Itô calculus could be used to determine the necessary value of  $\kappa$ , which related that martingale to a conformally invariant, continuous  $\text{SLE}(\kappa)$  curve. This is where the advantage of SLE was clearly evident. SLE connected a physical observable to a curve which was already conformally invariant by definition; in contrast, conformal field theory and the methods of the renormalization group sought to prove conformal invariance, something which they were never able to do. As a result SLE gave physicists the properties they wanted in their physical models but also satisfied mathematicians demanded for a natural and rigorous process. It was not long after SLE was invented that it started making an impact. One of SLE's most notable applications was in the context of the Ising model.

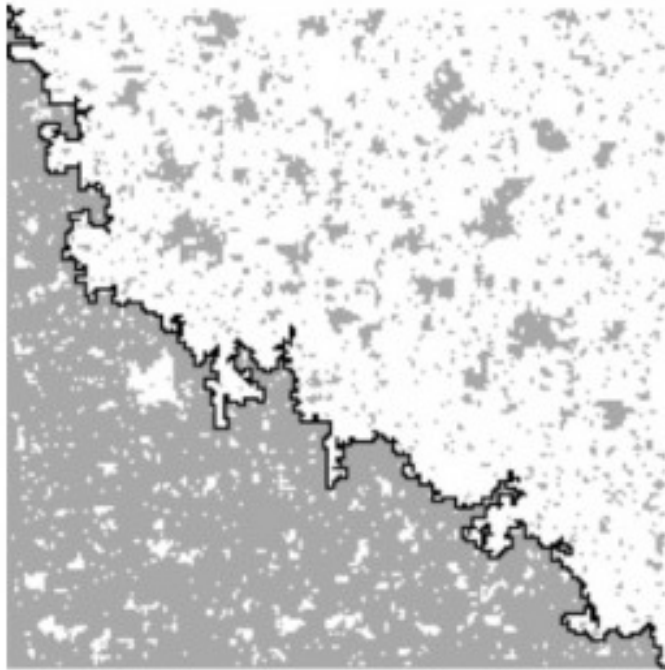


**Figure 3.6:** The SLE(3) curve as the Ising model domain wall, courtesy Stanislav Smirnov.

The application found success in the way the Ising model's martingale and observable were defined. To begin we assume the basic initial set up of the non-mean field theory Ising model as described in the Ising model section. The first step is to define the observable, which for this model is defined as the fermionic spin. A fermion is a fundamental particle and as such it has an intrinsic spin. The fermionic spin observable was defined by the celebrated mathematician Stanislav Smirnov and is based roughly on the winding number of the domain wall in the Ising model. It was a great achievement, accomplished by Stanislav Smirnov, to prove that the domain wall could be represented as the SLE(3) curve in [9], see Figure (3.6). For more details regarding SLE and its relationship to observables we refer the interested reader to the following additional sources for more information [3, 8, 9, 14, 17, 18].

# Chapter 4

## Crack Propagation Application

### 4.1 The Percolation Model

Now that we have seen the Ising model in detail, explored the need for SLE, and seen how it resolves both the desires of the physics community and the rigor of the mathematical community we can now look at a different model which inspired our application of crack propagation. The model we will now discuss is the percolation model.

The purpose of the percolation model is to model how a liquid percolates through a porous material. To achieve this, the model is first defined on any lattice where every tile is independently colored either white or black. In Figure (4.1) we show percolation on a hexangle lattice, with each tile having an equal probability of being either white or black, with the exception of the boundary tiles. The boundary tiles colors are fixed. There are several choices for boundary conditions but the ones we will use are known as Dobrushin boundary conditions. These boundary conditions fix half of the boundary tiles as white and the other half as black. The random assignment of black and white colors to the remaining tiles is what generates the stochastic nature of this model. The last aspect of this model that needs introducing is the exploration process and its resulting path. In order to replicate the process of a

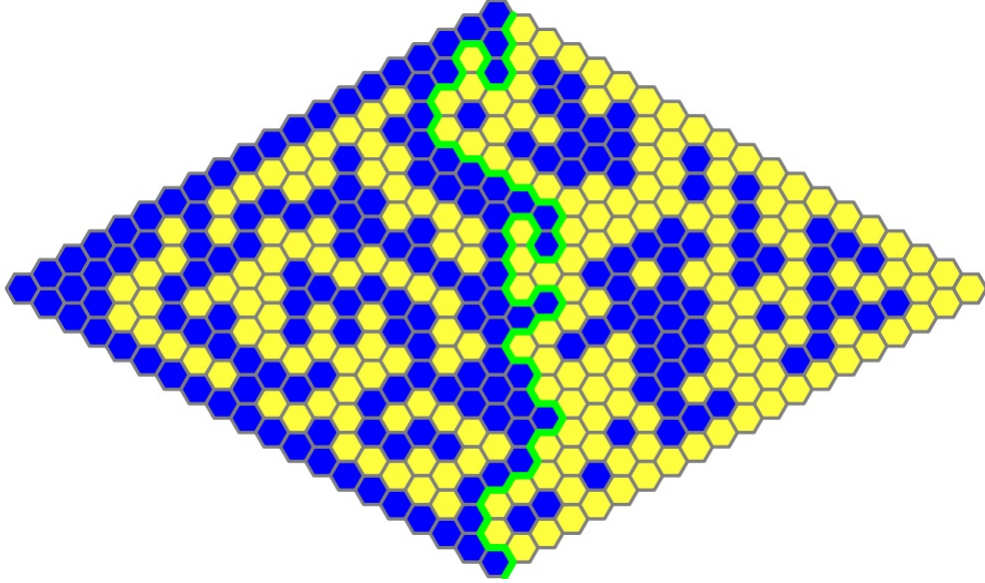


**Figure 4.1:** Percolation model image courtesy Tom Alberts

liquid percolating through this medium, a path must be defined. The path obeys the following law: the path must always have black tiles on one side and white tiles on the other. Following this rule a path is created which, under these boundary conditions, traverses the entire lattice. See Figure(4.1). This path was proven to converge to an SLE(6) process by Stanislav Smirnov, via the crossing probabilities and Cardy's formula. For more details on Smirnovs work, consult [2, 3].

## 4.2 Crack Propagation Simulations

The phenomena we wished to investigate were the evolution of cracks through heterogeneous materials. We hoped to use the percolation model as a analog for any variety of imperfect materials, and to investigate curves that modeled the path a crack would take as it progressed through a material. See Figure (4.2, 4.3). The nature of the cracks we hoped to model would be tearing in nature similar to the action of tearing a piece of paper. This tearing action led us to apply our boundary conditions to the initializing side of our model and nowhere else. We also assumed our crack would propagate laterally from left to right. The next step was to actually



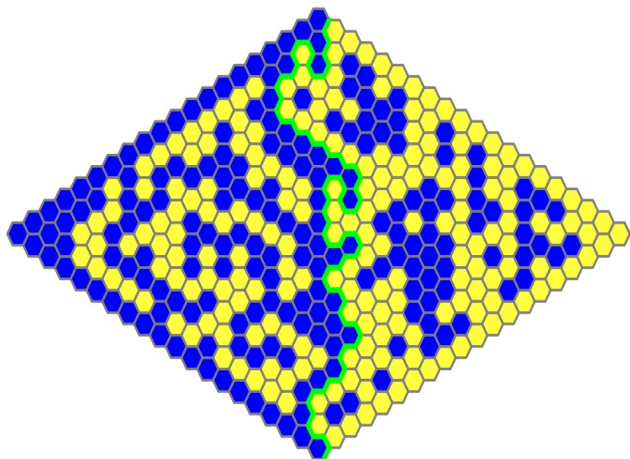


**Figure 4.2:** Percolation model representation



**Figure 4.3:** Crack process we hoped to model

see if the exploration process could be used to create a viable candidate for such a process.

### Initial Observations

After simulating the percolation process, we analyzed its behavior. In particular, we noted that the curve often created large meandering paths that looped back close to a past point on the path. See Figure (4.2). This obviously did not make much physical sense. Cracks moving across a material do not loop back on themselves under our tearing force assumption. Consequently, we wished to modify the percolation exploration process to give a more realistic result. After much experimentation, failed simulations, and false starts, a potential solution emerged.

### The Pinch Process

Our goal was to eliminate near closed loops created by the exploration process. The physical rationale was that we would allow the crack to break through a sufficiently small piece of material. In this context the breaks would only occur over black tiles. In other words only portions of black clusters could break-off or could be crossed. We programmed this, via Matlab code, by first following the exploration path; when the

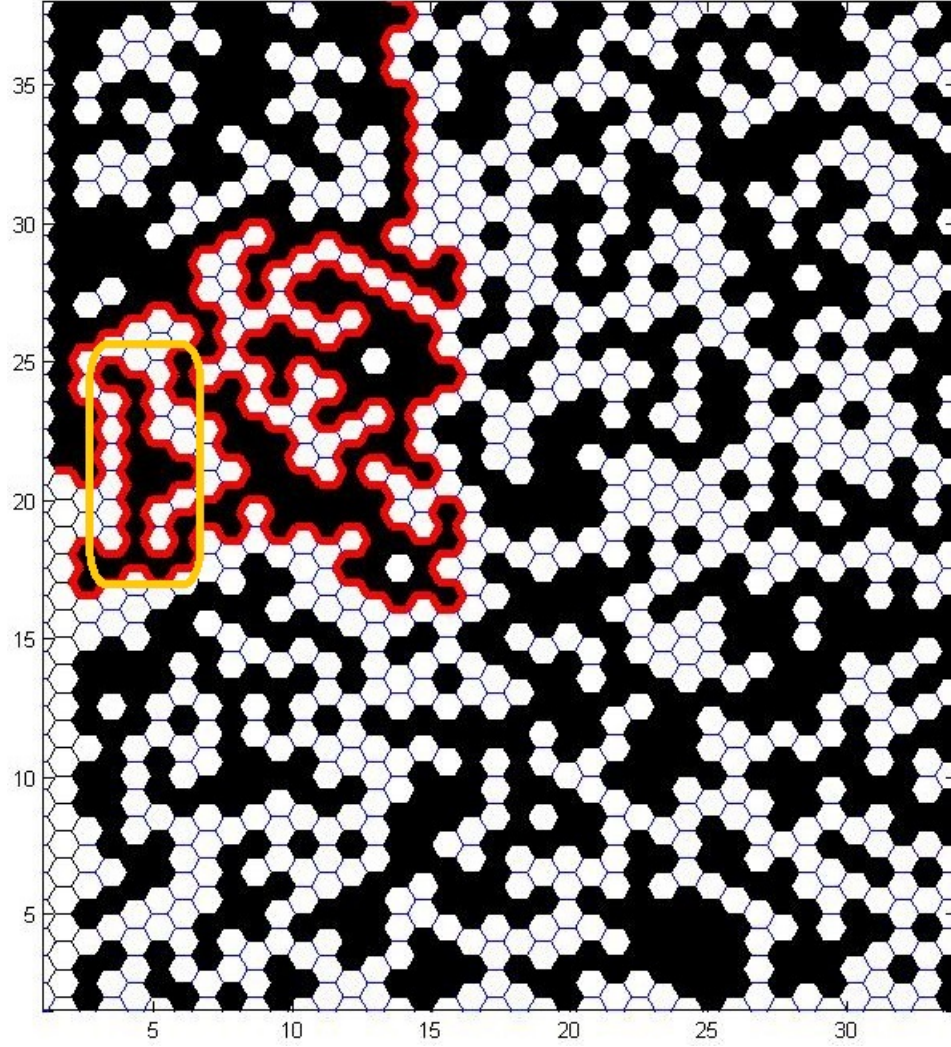


**Figure 4.4:** Failings of the percolation model.

exploration path came within one tile of a point it had already been, in the x-direction only, thus creating a near closed loop, we allowed the path to jump across the black tile containing those points. The result was a less meandering path without large near closed loops, which is exactly what we wanted. We ran a small scale simulation to test this idea, as seen in Figure (4.5). The resulting curve looked more promising than the pure exploration process due to its more directed travel across the lattice. The next step was to scale up the size of our lattice. The larger scale simulation preformed as expected and was successful regardless of the distribution of black and

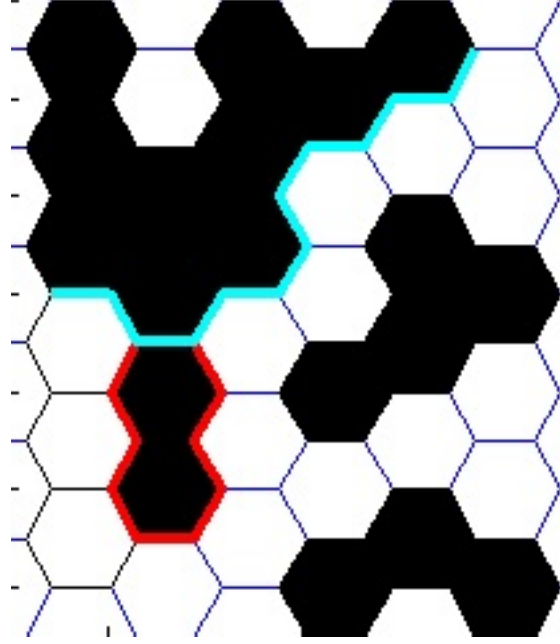


**Figure 4.5:** Small scale pinch process.

white tiles. See Figures (4.6, 4.7). It is important to note this algorithm takes effect only if a loop is created by the exploration path. If the exploration process proceeds across the lattice in a linear fashion, with no loops created, the algorithm is not used.

## Future Work

Numerous interesting questions emerged from these simulations, such as: Is this new curve an SLE process, or related to one? Both of these question are far outside the scope of this paper, and I hope others interested in this area will explore it further. Additionally, other modifications could be made to explore our pinch process further. Allowing the curve to jump over both white and black tiles is one such modification. Another idea to investigate is the nature of local processes and global results. We toyed with several different locally driven algorithms, most of which resulted in global results which were not as we desired. The natural next question is whether certain local rules can create a process that better models the crack propagation.

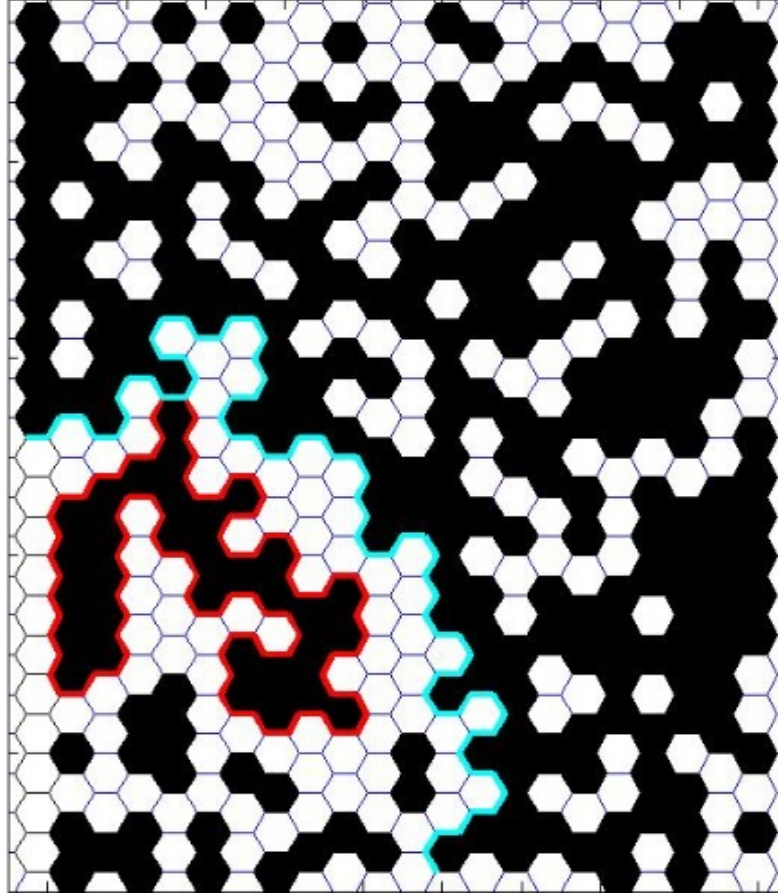


**Figure 4.6:** Large scale pinch process.

The next physical step in our analysis is to compare our results with some real world data. When working in an applied setting the ultimate test of a theoretical model is its validity with experimental data, and as of now, we have yet to carry out such a comparison.

In addition to the more mathematical questions, we see many other places SLE could potentially be applied as well. The relationship between curves created by electronic discharge and SLE, the outline of clouds and their evolution, are just a few potential places SLE may prove to provide additional insight.



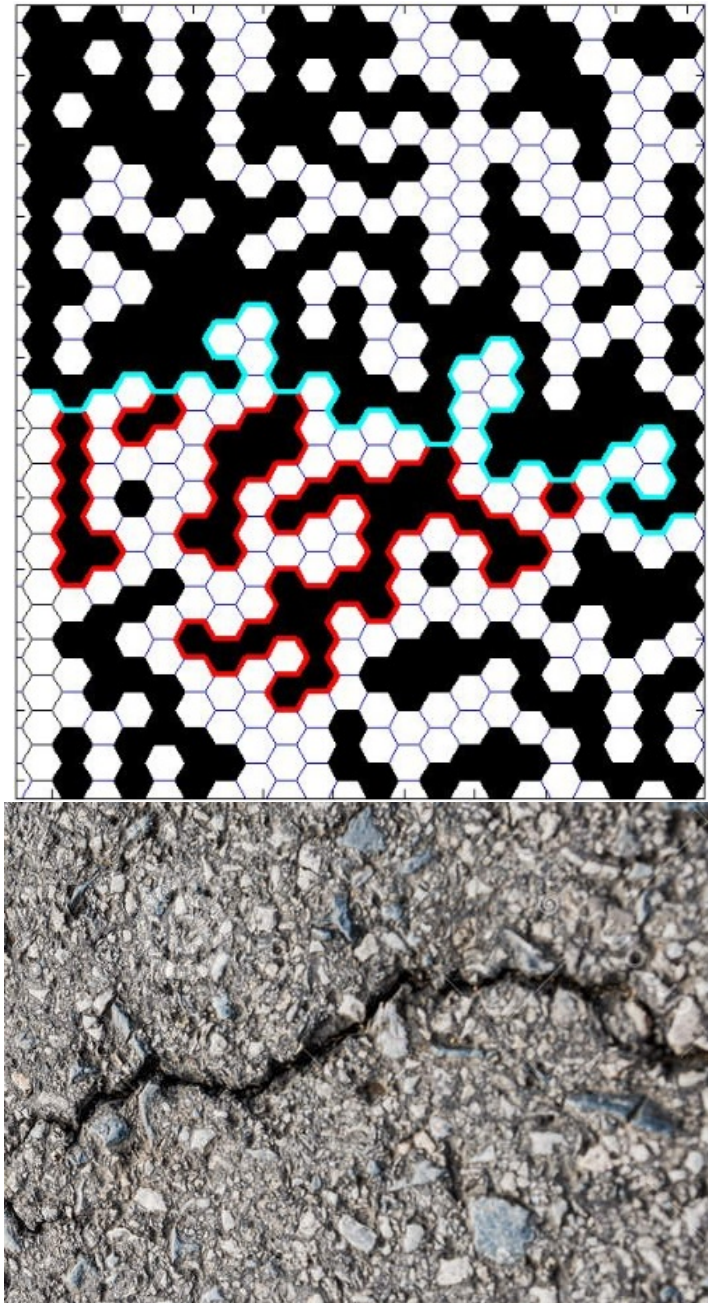


**Figure 4.7:** Large scale comparison.

# Chapter 5

## Conclusions

We have covered a very broad range of topics in this thesis, and in a very broad manner. If successful, the reader should now understand many things about the physical origins and motivations of SLE. We began with the study of phase transitions at its most fundamental level with the Ideal Gas Law. This simple mathematical expression then evolved into a more complicated and accurate model in the Van der Waals equation. These models and their implications highlighted the importance of critical exponents as they relate to the order parameters of statistical mechanical models. In particular, we discussed the details of the Ising model and if this section of the thesis was a success then the reader should now possess a basic working knowledge of the Ising model and consequently many other two dimensional lattice models. The new found insight that resulted from the Ising model allowed for the powerful and accurate mathematical tools the renormalization group and conformal field theory to be applied, where they significantly improved the accuracy of critical exponents. We then saw the limits of these new methods, directly motivating SLE's creation. The most important outcome of this section is the reader's exposure to statistical mechanics and understanding its motivation and connection to SLE.

The second outcome of this thesis was a basic introduction to SLE and its relevant concepts. Several topics in probability were discussed including Brownian motion,

random walks, and martingales. We then saw how these concepts are utilized in SLE and in a slightly more mathematical tone, how the probabilistic details of SLE tie back into certain physical models.

The final outcome of this thesis was to introduce and explore a potential new model of crack propagation processes. We succeeded in implementing our proposed model in the form of the pinching process. Initial results suggest that this process holds potential in this application, but needs additional analysis to confirm that hope. Additionally, several important questions came out of our simulations. These questions involve most notably, the relationship between local processes, global results, and the relevant SLE processes. The most important outcome of this entire thesis is to spark curiosity, to encourage new ideas and perspectives, ultimately leading to a better understanding of this subject and those directly related to it.

# Bibliography



- [1] Binney, J. J., Dowrick, N., Fisher, A., and Newman, M. (1992). *The theory of critical phenomena: an introduction to the renormalization group*. Oxford University Press, Inc. 23
- [2] Camia, F. and Newman, C. M. (2007). Critical percolation exploration path and sle 6: a proof of convergence. *Probability theory and related fields*, 139(3-4):473–519. 37
- [3] Cardy, J. (2005). Sle for theoretical physicists. *Annals of Physics*, 318(1):81–118. 35, 37
- [4] Chaikin, P. M. and Lubensky, T. C. (2000). *Principles of condensed matter physics*, volume 1. Cambridge Univ Press. 13
- [5] Cipra, B. A. (1987). An introduction to the ising model. *American Mathematical Monthly*, 94(10):937–959. 10, 13
- [6] De Branges, L. (1985). A proof of the bieberbach conjecture. *Acta Mathematica*, 154(1):137–152. 1
- [7] Donsker, M. D. (1951). An invariance principle for certain probability limit theorems. AMS. 28
- [8] Duminil-Copin, H. (2013). Parafermionic observables and their applications to planar statistical physics models. *Ensaïos Matemáticos*, 25:1–371. 13, 23, 24, 35
- [9] Duminil-Copin, H. and Smirnov, S. (2012). Conformal invariance of lattice models. *Preface vii Schramm-Loewner Evolution and other Conformally Invariant Objects 1 Vincent Beffara Noise Sensitivity and Percolation 49*, page 213. 15, 35
- [10] Gaberdiel, M. R. (2000). An introduction to conformal field theory. *Reports on Progress in Physics*, 63(4):607. 24
- [11] Guggenheim, E. A. (1945). The principle of corresponding states. *The Journal of Chemical Physics*, 13(7):253–261. 6, 7

- [12] Hill, T. (1960). An introduction to statistical thermodynamics, p289, addison. 6
- [13] Karatzas, I. (1991). *Brownian motion and stochastic calculus*, volume 113. springer. 30
- [14] Lawler, G. F., Schramm, O., and Werner, W. (2011). Conformal invariance of planar loop-erased random walks and uniform spanning trees. In *Selected Works of Oded Schramm*, pages 931–987. Springer. 35
- [15] McMillan, W. (1984). Domain-wall renormalization-group study of the two-dimensional random ising model. *Physical Review B*, 29(7):4026. 23
- [16] Pelissetto, A. and Vicari, E. (2002). Critical phenomena and renormalization-group theory. *Physics Reports*, 368(6):549–727. 20
- [17] Rohde, S. and Schramm, O. (2011). Basic properties of sle. In *Selected Works of Oded Schramm*, pages 989–1030. Springer. 33, 35
- [18] Schramm, O. (2011). Conformally invariant scaling limits: an overview and a collection of problems. In *Selected Works of Oded Schramm*, pages 1161–1191. Springer. 35
- [19] Zumdahl, S. and DeCoste, D. J. (2012). *Chemical principles*. Cengage Learning. 6, 7

# Appendix

# Matlab Code

```
clear all

%%%%%%%%%%%%%%%%%%%%%%%%%%%%%%%%%%%%%%%%%%%%%%%%%%%%%%%%%%%%%%%%%%%%%%%% create lattice %%%
MG = 24;          %MG-2= number of XY columns/rows
HP = (MG/2)+1;    %Half-way point
[X Y]= meshgrid(1:1:MG);
n = size(X,1);
X = sqrt(3)/2 * X;
Y = Y + repmat([0 1/2],[n n/2]);
figure(1);

voronoi(X(:),Y(:));
[VX VY] = voronoi(X(:),Y(:));
plot(VX,VY,'-b');
axis equal, axis([1 34 1.5 38]);

dt = delaunayTriangulation(X(:),Y(:));
%dt = DelaunayTri(X(:),Y(:));
%hold on;
%triplot(dt,'-r');
%hold off;
```

```

tidx = dt.pointLocation(2,4);
cc = dt.circumcenter(tidx);
%hold on;
%plot(cc(1),cc(2),'o g','MarkerSize',25);
%hold off;

LY = zeros(size(Y,1),1);

for i = 1:size(Y,1)          %LY is my y-cord for line
    LY(2*i-1,1) = Y(i,1);
    LY(2*i,1) = Y(i,2);

end

VT_1 = zeros(size(LY,1)-1,2);%begin to find boundry verts
    %VT_1 are the left verts

for j = 1:size(LY,1)-1;
    tidy = dt.pointLocation(1.4434,LY(j,1));
    VT_1(j,:) = dt.circumcenter(tidy);
end

VT_2 = zeros(size(LY,1)-1,2); %VT_2 are the right verts

for j = 1:size(LY,1)-1;
    tidy = dt.pointLocation(2.0207,LY(j,1));

```

```

        VT_2(j,:) = dt.circumcenter(tidy);
    end
    %%%%%%%%% end work to find boundry vertices

    VT_end = zeros(size(LY,1)-1,2); %VT_2 are the right verts

    for j = 2:size(LY,1)-1;
        endy = dt.pointLocation(X(1,MG),LY(j,1));
        VT_end(j,:) = dt.circumcenter(endy);
    end

    [V,R] = voronoiDiagram(dt);
    m = size(R(:));
    m = m(1,1);

    %%%%%%%%% begin random tile test

    RV = rand(m,1); %random number comparison vector
    WT = cell(m,1); %cells for white tile index data

    for i = 1:m
        if RV(i,1) > .5
            WT{i} = R{i};
        end
    end
end

```

```

for i = 1:m
    if length(WT{i}) < 6;
        WT{i} = [];

    end

end

WT(any(cellfun(@isempty,WT),2),:) = [];
WT = cell2mat(WT);

for j = 1:m
    if RV(j,1) > .5
        R{j}=0;
    end
end

for i = 1:m
    if length(R{i}) < 6;
        R{i} = [];

    end

end

R(any(cellfun(@isempty,R),2),:) = [];

```

```

%%%%%%%%%%%%%%%%%%%%%%%%%%%%%%%%%%%%%%%%%%%%%%%%%%%%%%%%%%%%%%%%%%%%%%%% prepare data to patch

BT = cell2mat(R);           %convert cells into matrix
SV = 6*size(BT,1);         %number of vertices
SR = size(BT,1);           %number of faces
verts = zeros(SV,2);       %preallocate vertex storage
zdata = ones(6,SR);
faces = zeros(SR,6);

for j = 1:SR
    for i = 1:6
        faces(j,i) = (j-1)*6 + i;
    end
end

for i = 1:size(BT)
    for j = 1:6
        RR((i-1)*6 + j) = BT(i,j);
    end
end

for v = 1:SV;
    verts(v,:) = V(RR(v),:);
end

p = patch('Faces',faces,'Vertices',verts,'FaceColor','k');

```



```
%%%%%%%%%%%%%%%%%%%%%%%%%%%%%%%%%%%%%%%%%%%%%%%%%%%%%%%%%%%%%%%%%%%%%%%%boundary condition tiles
```

```
P = (size(VT_1,1)-3)/2;
```

```
numberBlackTiles = P/2;
```

```
Bverts = zeros(numberBlackTiles,2);
```

```
q = numberBlackTiles ;
```

```
j = size(VT_1,1);
```

```
for i = 1:q
```

```
    Bverts(1+6*(i-1),:) = VT_2(j,:);
```

```
    Bverts(2+6*(i-1),:) = VT_1(j,:);
```

```
    Bverts(3+6*(i-1),:) = VT_1(j-1,:);
```

```
    Bverts(4+6*(i-1),:) = VT_1(j-2,:);
```

```
    Bverts(5+6*(i-1),:) = VT_2(j-2,:);
```

```
    Bverts(6+6*(i-1),:) = VT_2(j-1,:);
```

```
    if j-2 > q
```

```
        j =j-2;
```

```
    else
```

```
        break
```

```
    end
```

```
end
```

```
Bfaces = zeros(q,6);
```

```
for j = 1:q
```

```
    for i = 1:6
```

```

        Bfaces(j,i) = (j-1)*6 + i;
    end
end

bzdata = ones(6,q);

Bp = patch('Faces',Bfaces,'Vertices',Bverts,'FaceColor','k');

BWverts = zeros(6*q,2);
w=3;

for i = 1:q
    BWverts(1+6*(i-1),:) = VT_2(w+2,:);
    BWverts(2+6*(i-1),:) = VT_1(w+2,:);
    BWverts(3+6*(i-1),:) = VT_1(w+1,:);
    BWverts(4+6*(i-1),:) = VT_1(w,:);
    BWverts(5+6*(i-1),:) = VT_2(w,:);
    BWverts(6+6*(i-1),:) = VT_2(w+1,:);

    if w+2 <= (size(VT_1,1)+3)/2;
        w = w +2;
    else
        break
    end
end

BWfaces = zeros(q,6);

for j = 1:q

```

```

        for i = 1:6
            BWfaces(j,i) = (j-1)*6 + i;
        end
    end

    end

    bwzdata = ones(6,q);

    BWp=patch('Faces',BWfaces,'Vertices',BWverts,'FaceColor','w');

    VVT_1 = zeros(1/2*(size(VT_1,1)-1),2);

    for i = 1:(size(VT_1,1)-1)/2
        VVT_1(i,:) = VT_1(2*i,:);
        if VVT_1(i,2) > HP
            upperhalf(i,:) = VVT_1(i,:);
        else
            lowerhalf(i,:) = VVT_1(i,:);
        end
    end

    end

    lowerhalf(1,:) = [];
    upperhalf(~any(upperhalf,2), :) = [];

    Iupperhalf = zeros(size(upperhalf,1),1);

    %Iupperhalf is row index of unique boundry verts above HP

    for j = 1:size(upperhalf,1)
        for i = 1:size(V,1)

```

```

        vvt_1c = abs(V(i,:)- upperhalf(j,:));
        if vvt_1c < 0.001
            Iupperhalf(j) = i;
        end
    end
end

Ilowerhalf = zeros(size(lowerhalf,1),1);

%same thing as Iupperhalf just for lower vertices

for j = 1:size(lowerhalf,1)
    for i = 1:size(V,1)
        vvt_1c = abs(V(i,:)- lowerhalf(j,:));
        if vvt_1c < 0.001
            Ilowerhalf(j) = i;
        end
    end
end

end

%%%%%%%%%%%%%%%%%%%%%%%%%%%%%%%%%%%%%%%%%%%%%%%%%%%%%%%%%%%%%%%%%%%%%%%% trial for exploration data

BT(:,7) = 1;
WT(:,7) = 0;

%creates 7th column in BT,WT to distinguish

Hex = [BT;WT];

```

```

BIhex = {size(Iupperhalf,1)};
for i = 1:size(Iupperhalf,1) %cell contains
    [a b] = find(Hex == Iupperhalf(i));%indx for rows
    BIhex{i} = [a b]; %for vertex in certain hex
end

for i = 1:size(Iupperhalf,1)
    Hex(BIhex{i}(1,1),7)= 1;
end

LBIhex = {size(Ilowerhalf,1)};

for i = 1:size(Ilowerhalf,1)
    [e f] = find(Hex == Ilowerhalf(i));
    LBIhex{i} = [e f];
end

for i = 1:size(Iupperhalf,1)
    Hex(LBIhex{i}(1,1),7) = 0;
end

UBindex = zeros(size(VVT_1,1),1);
for j = 1:size(upperhalf,1)
    for i = 1:size(V,1)
        if abs(upperhalf(j,:) - V(i,:)) < 0.01
            UBindex(i,1)= i;
        end
    end
end

```

```

end

UBindex( ~any(UBindex,2), : ) = [];

LBindex = zeros(size(VVT_1,1),1);


I = intersect(WT,BT);           %common w & b verts
ExpData = zeros(size(I,1),2); %preallocate


IP = [2.0207,HP]; %create intial conditions%
Path = zeros(size(ExpData,1),2);%           ''      %
Path(1,:) = [1.4434,HP]; %           ''      %
Path(2,:) = IP; %           ''      %
u = 3;           %           ''      %
Dist = zeros(size(V(:,1),1),1); % preallo Dist mat


while(u < size(ExpData,1))

```

```

for i = 1:size(V(:,1),1) %for loop to find
    XX = [Path(u-1,:);V(i,:)]; %distance from path
    Dist(i,1) = pdist(XX,'euclidean');%& all verts
end
q=1;
Three = zeros(3,2); %Holds the 3 nearest pts
for i = 1:size(V(:,1),1)
    if Dist(i,1) > 0.01 && Dist(i,1)<0.6
        Three(q,:) = V(i,:);
        q = q+1;
    end
end

for i = 1:3
    ccc = abs(Three(i,:) - Path(u-2,:));%potential pts
    if sum(ccc) < 0.01
        Three(i,:)= [];
        break
    end
end

IV = zeros(2,1);
for j = 1:2
    for i =1:size(V,1)
        cv = abs(Three(j,:) - V(i,:));
        if sum(cv) < 0.01;
            IV(j) = i;
            break
        end
    end
end

```

```

end
end

for i = 1:size(V,1)
    ccv = abs(Path(u-1,:)- V(i,:));
    if sum(ccv) < 0.01;
        IV(3) = i;
        break
    end
end

Points = {3*size(IV,1),2};
for i = 1:size(IV,1)
    [c d] = find(Hex == IV(i));
    Points{i} = [c d];
end

G = intersect(Points{1}(:,1),Points{2}(:,1));
K = intersect(Points{2}(:,1),Points{3}(:,1));
H = intersect(Points{1}(:,1),Points{3}(:,1));
commontile = intersect(G,H);

if isempty(commontile)== 1; %stop the path when
    break    %comparison fails
end

P1 = Points{1}(find(Points{1}(:,1)~=commontile));
P2 = Points{2}(find(Points{2}(:,1)~=commontile));

```



```

P3 = Points{3}(find(Points{3}(:,1)~=commontile));

KK = intersect(P2,P3);
HH = intersect(P3,P1);
comparetiles = [KK;HH];

for i = 1:size(comparetiles,1)
    if Hex(commontile,7)+Hex(comparetiles(i,1),7) == 1

Path(u,:) = Three(1,:);
    else Path(u,:) = Three(2,:);
    end
end

u = u + 1;
end

Path( ~any(Path,2), : ) = [];

hold on
plot(Path(:,1),Path(:,2),'r','linewidth',3)
hold off

%%%%%%%%%%%%%%%%%%%%%%%%%%%%%%%%%%%%%%%%%%%%%%%%%%%%%%%%%%%%%%%%%%%%%%%% Begin Loop-Erased Path

LEpath(1,:) = Path(1,:);

```

```

LEpath(2,:) = Path(2,:);

jj = 2;
ii = 2;

temp = zeros(2,1); %stores row hex index

while jj < size(Path(:,1),1)+1

DD = zeros(size(Path(:,1),1)-jj,1);

    for kk = jj+1: size(Path(:,1))
        DD(kk-jj) = abs(LEpath(ii,2)-Path(kk,2));
    end

EE = find( DD < 0.1);

    if sum(EE) < 0.01
        LEpath(ii+1,:) = Path(jj,:);
        ii = ii+1;
        jj= jj+1;
    else
        FF = Path(EE(1)+jj,:);

        if abs(FF(1,1) - LEpath(ii,1)) < .65

%check hex%%%%%%%%%%

```

```

        for kk = 1:size(V,1)
            if abs(V(kk,1)-FF(1,1)) < 0.01 &&
abs(V(kk,2)-FF(1,2)) < 0.01
                temp(1) = kk;
            end
        end

        for kk = 1:size(V,1)
            if abs(V(kk,1)-LEpath(ii,1))< 0.1 &&
abs(V(kk,2)-LEpath(ii,2)) < 0.1
                temp(2) = kk;
            end
        end

        [row,col] = find(Hex == temp(1));
        AA = [row];
        [row,col] = find(Hex == temp(2));
        BB = [row];

        CC = intersect(AA,BB);
        if (Hex(CC(1),7)+ Hex(CC(2),7))< 2.1 &&
(Hex(CC(1),7)+ Hex(CC(2),7))> 1.9
            LEpath(ii+1,:)= FF(1,:);
            ii = ii+1;
            jj = EE(1)+jj;
        else LEpath(ii+1,:) = Path(jj,:);
            jj = jj+1;
            ii = ii+1;

```

```

end

%%%%%%%%%%%%%%%%%%%%%%%%%%%%%%%%%%%%%%%%%%%%%%%%%%%%%%%%%%%%%%%%%%%%%%%%

else
    LEpath(ii+1,:) = Path(jj,:);
    ii = ii+1;
    jj= jj+1;
end
end
end

hold on
plot(LEpath(:,1),LEpath(:,2),'c','linewidth',3);
hold off

```

# Vita

Christopher Mesic was born and raised in Sacramento, California. After finishing high school Christopher attended Oregon State University for two years, where he studied biological anthropology. Christopher continued his education at the University of California at Santa Cruz, where after briefly studying geophysics, he ultimately graduated in 2010 with a B.A. in mathematics. After studying abroad and working for two years, Christopher was accepted as a masters student to the University of Tennessee at Knoxville where he planned to advance his mathematics education. Upon graduation, Christopher plans to put his new found degree and education to work in industry.